A REMOTE SENSING APPROACH FOR ESTIMATING BANK STRENGTH AND PERCENT VEGETATIVE VOLUME ON TEXAS STREAMBANKS

A Thesis

by

JACQUELINE E. RAMBO

Submitted to the Office of Graduate and Professional Studies of
Texas A&M University
in partial fulfillment of the requirements for the degree of

MASTER OF SCIENCE

Chair of Committee,	Ronald Kaiser
Co-Chair of Committee,	Fouad Jaber
Committee Members,	Diane Boellstorff
Head of Department,	Ronald Kaiser

May 2021

Major Subject: Water Management and Hydrological Science

ABSTRACT

The total approximate in-stream damage from erosion has been calculated at $5 billion for the United States each year, with a minimum of $15 billion spent on stream restoration within the United States from 1990 to 2005 (Bernhardt et al., 2005). Planting riparian vegetation is one of the techniques used to stabilize streambanks during stream restorations, but few data exist evaluating the quantitative effect of various plant species on bank stabilization. This study aims to clarify the role of vegetation on bank stabilization in Texas streams. This relationship is shown herein by calculating bank strength values using channel geometry equations and USGS stream discharge data, and correlating those values to an estimation of the percentage of the bank area's vegetative volume. Vegetation cover along several streams in Texas was calculated using a bare-earth DEM and a LiDAR point cloud at each USGS stream gauge location using Google Earth Engine®. The bank strength of each stream was calculated along a cross section that intersects the USGS stream gauge. At that location, a buffer was generated around that location to collect the percent volume of vegetation (PVV) on the streambank; vegetation type was separated into 3 categories: low, medium, and high. The buffer's radius was wide enough to account for the root extent of a live oak, the study region's tallest tree. Results from this research found that higher concentrations of the "high" vegetation were associated with relatively higher bank strengths in sand, clay or mud streams. Additionally, higher concentrations of low and medium vegetation were found to be associated with relatively lower bank strengths in sand, clay or mud streams. There

was no change in bank strength when varying volumes of vegetation were analyzed amongst limestone streams. Additionally, this study represents the first calculated coefficients of critical shear stress that correspond to numerical measurements of high vegetation. Knowing the quantitative impact of vegetation may help stream restoration planners decide on an appropriate vegetation volume needed to stabilize streambanks in Texas. This thesis proposes an innovative means of understanding the important relationship, and the quantitative effect, between different vegetation volumes on streambank strengths.

DEDICATION

I would like to dedicate this thesis to my sister, Sierra. As you start your college adventures next year, I hope you find that one hobby or study that brings you joy like no other, and I hope it makes you excited to wake up every morning, or perhaps afternoon since you'll likely be a typical college kid ☺.

ACKNOWLEDGEMENTS

I would like to thank my committee chair, Dr. Kaiser, committee co-chair, Dr. Jaber and committee member, Dr. Boellstorff, for their guidance and support throughout the course of this research and for providing helpful feedback and edits. For the kindness and exuberance that was poured into the knowledge shared, and for his tireless dedication of time ensuring our weekly meetings were maintained, I owe special thanks to Dr. Jaber. Thanks also go to my friend and co-worker, Luna Yang, for her help with teaching me the process of modelling bankfull discharge in rivers and streams. I would also like to thank Derek Cheung and Ben Grunau for dedicating their day to help me collect stream profiles in the field. Their work is immensely appreciated, and they've been incredibly supportive throughout this whole process. Additionally, I would like to thank Lucas Gregory at the Texas Water Resources Institute who was very helpful in lending me the survey equipment needed to collect stream profiles to ground truth my stream profile generator. Thanks also goes to my Mom for driving my Grandma's soup to my roommates and me when we were writing our theses. We probably would not have eaten if it weren't for her. The appreciation I have for my mother's care, love, and support more than I can even express. Thanks also goes to my sister, Sierra, who kept saying "you got this!" It truly gave me the motivation to keep going. Thank you to my Dad and Tia Anna as well, for initially instilling my love of science and curiosity at such a young age. Thank you also goes to Ben's parents, George and Lori, for all the encouraging words and food! Finally, the biggest thanks of all goes to my partner, Ben, for being the constant source of light and

support in my life. I think I would have been 20 times more depressed, in the same way that an amount of 40% high vegetation can increase the critical shear stress by 20 times, Ben, you have increased my happiness in life by 20 times if I could put a number on it, but we all know that the appreciation I have for you is immeasurable.

CONTRIBUTORS AND FUNDING SOURCES

Contributors

This work was supervised by a thesis dissertation committee consisting of Professor Ronald Kaiser of the Department of Range, Wildlife and Fisheries Management as Chair, Professor Fouad Jaber of the Department of Biological and Agricultural Engineering as Co-Chair and Professor Diane Boellstorff of the Department of Soil and Crop Sciences as committee member.

Funding Sources

This study was partially funded by a 319(h) nonpoint source pollution grant provided by the Texas Commission on Environmental Quality (TCEQ) and the US Environmental Protection Agency (EPA).

NOMENCLATURE

b	basal width of stream profile
C_w	bank strength coefficient
D	depth
DEM	Digital Elevation Model
d_i	largest particle from the bar sample
d_{50}	median diameter of particles on the wetted perimeter
$d^{\wedge}_{50}$	median diameter of particles on the bar sample
LPC	Lidar Point Cloud
n	Manning's roughness coefficient
NCD	Natural Channel Design
NRCS	Natural Resources Conservation Service
PVV	Percent Volume of Vegetation
Q	bankfull discharge
R	hydraulic radius of the riffle cross-section at bankfull stage
S	water surface gradient or slope
τ_{cbk}	bank strength
τ_c	critical shear stress
τ	shear stress
USGS	United States Geological Survey
γ	density of water
W	width

z	slope of the sides of the stream profile

TABLE OF CONTENTS

Page

LIST OF FIGURES

Page

LIST OF TABLES

Page

1. INTRODUCTION

Streambank erosion is a major cause of excess sediment and pollutants that enter lakes, reservoirs, ponds, and downstream channels, reducing reservoir storage capacity and increasing the cost to treat drinking water. Streambank erosion is a natural process, but direct human activities, such as land use change and channel confinement or realignment, can cause the frequency and magnitude of water forces to increase; loss of vegetation can also cause the streambanks to become more susceptible to erosion (Klausmeyer, n.d.). Changes in land use that increase surface runoff can also dramatically increase in-stream peak discharge, which can further increase streambank erosion (Childers, 2010). The increased sediment load in streams adversely affects fish habitats by causing changes in pool quality, substrate materials, imbrication, and other physical habitat loss. In addition to the impact on riparian ecosystems and reservoirs, streambank erosion also impacts floodplain residents, bridges, and other streamside structures (ASCE, 1998). If these structures are located on or near the streambank, they are at risk of falling into the stream channel by way of streambank retreat, which typically occurs by a combination of subaerial processes and erosion, fluvial erosion, and bank failure (Lawler, 1995). If the appropriate precautions are made, the damages from streambank erosion can be mitigated.

A channel is considered "stable" when it has the ability to maintain its dimensions, pattern, and profile without either aggrading, degrading, incising, widening, or narrowing. (Rosgen, 1994). A stable channel has the liberty to adjust to a wide range of flows and

sediment inputs, but ultimately, the channel should promptly reach an equilibrium state where the amount of sediment that is coming into the channel should be the same amount that is flowing out of it. The U.S. Army Corps of Engineers (Fripp et al., 2011) suggests a wide variety of techniques that can be applied when restoring a stream to a stable state that minimizes streambank erosion. This often includes the use of planted vegetation as a form of bank protection. Beeson and Doyle (1995) in a study of river bends concluded that non-vegetated riparian bends were five times more likely than vegetated river bends to have undergone detectable erosion, and major bank erosion was thirty times more prevalent on non-vegetated bends than vegetated bends. The planting of vegetation is a proven technique because vegetation can increase boundary roughness, which in turn can decrease in-stream velocity and its potential to erode the streambank. As further justification for the use of vegetation in reducing the shear force of the stream or river, Hopkinson and Wynn (2009) showed that shrub and grass vegetation on the streambank decreased near-bank stream velocity by 43% and 66%, respectively. This study by Hopkinson and Wynn (2009) was conducted in a flume setting, where the results are heavily simplified due to the exclusion of other factors that contribute to stream velocity, such as the varying size and material of particles on a stream bank, as well as the variability of shape and slope that exists among streams. The root structure of vegetation along streambanks also provides strong cohesion for the bank material, reducing the critical shear stress, or the shear stress at which boundary sediments become entrained in the stream flow (Beeson and Doyle, 1995).

The shape of a channel is often used as an indicator of stream health and channel stability. Factors, such as slope and particle size, generally influence stream geometry, but the addition or omission of vegetation can also affect the stream's shape. Banks densely vegetated with deep-rooted species have narrower and deeper channels than those with thinly vegetated, grassy banks (Hey and Thorne, 1986). Others have also shown that forested streams are narrower than streams with herbaceous buffers (Gregory and Gurnell, 1988). There is a way to quantify how deep or entrenched a channel is. Rosgen (1994) defined channel entrenchment as the ratio between flood-prone width and channel bankfull width. Flood-prone width is the width of the floodplain at an elevation two times the maximum bankfull depth. Channels are defined as either entrenched, moderately entrenched, or slightly entrenched. The Forest Service Stream-Simulation Working Group uses the entrenchment ratio as an indicator of potential site risks associated with future alignment changes; slightly entrenched channels tend to undergo alignment changes as they shift across the flood plain (Gubernick et al., 2008). A visual representation of the stream geomorphology is shown in Fig. 1 below.

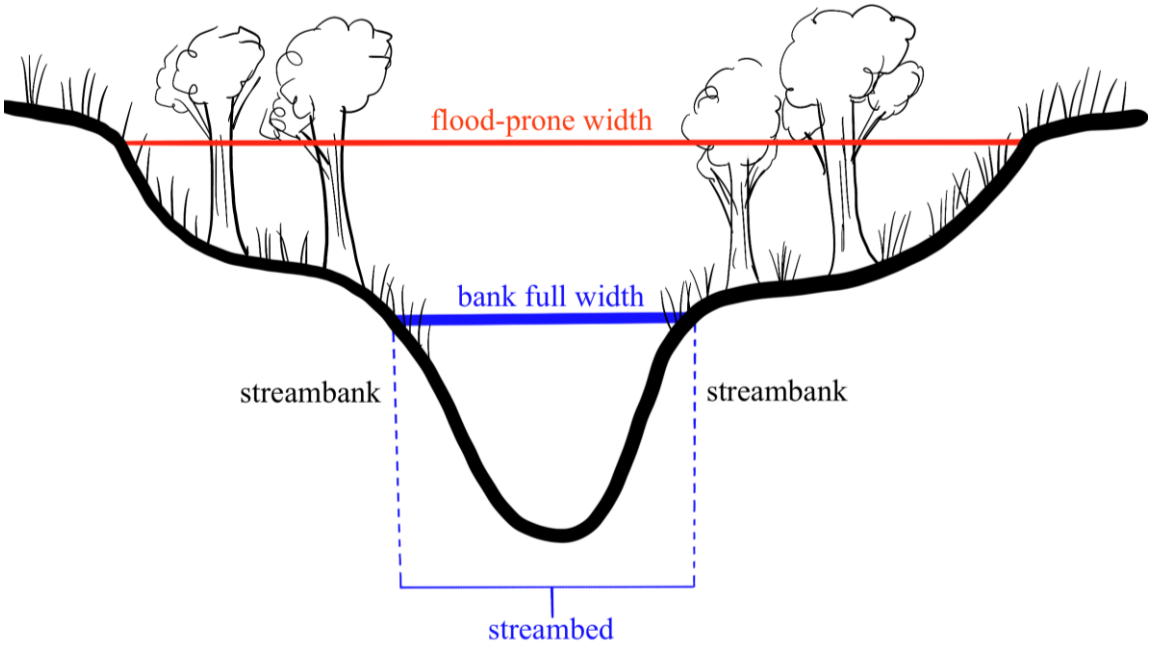

Figure 1. Cross-sectional view of stream geomorphology

Despite the common patterns between stream dimensions and an associated vegetative cover, there is still discrepancy amongst the patterns shown. Researchers have noted that streams were 2-2.5 times wider with forested riparian buffers than with grass buffers (Zimmerman et al., 1967), which contradicts many other studies (Hey and Thorne 1986, Gregory and Gurnell, 1988). The observed differences could be due to differing bank material across studies. Channels with cohesive banks have narrower and deeper channels than channels with non-cohesive banks (Knighton, 1998). Ultimately, the influence of vegetation on stream geometry is highly variable, and it also depends on what type of vegetation is used, since the root system varies depending on the plant species. Despite the highly variable nature of riparian vegetation and its effect on stream bank stability, it is certain that vegetation has a quantifiably positive effect on reducing

streambank erosion. The root systems of woody and herbaceous plants physically bind bank soils in place (Fig. 2), increasing the critical shear stress, or the minimum stress that is needed to move particles on the channel boundary (Gray and Leiser, 1982; Coppin and Richards, 1990; Thorne et al., 1997).

Figure 2. View looking downstream at USGS station 08159000. The exposed tree roots can be seen on the streambank, illustrating the binding effect that they have on the streambank sediments. This photo was taken in March 2021.

Some may note that the weight of added vegetation may promote bank retreat via mass wasting; however, Abernethy and Rutherfurd (2000) showed that vegetation does not contribute to bank destabilization. This is because plants undeniably enhance bank strength by reducing pore-water pressures and by directly reinforcing bank material with their roots.

Although it is certain that vegetation minimizes streambank erosion, the quantitative extent of this circumstance is unclear, which drives researchers to find

alternative or tangent methods of calculating the influence of vegetation on stream bank stability. Bank strength is a way to quantify a river or stream's bank stability. Bank strength has an influence on channel width, depth, and cross-sectional area, and therefore these parameters can be used to determine a stream's bank stability. In order to assess the integrity of a river or stream, the empirical relationship between bankfull channel geometry and discharge estimates has been shown to be a useful step in the process (McCandless, 2003). Bankfull discharge is the maximum discharge the channel can contain before the discharge overflows the streambanks and into the floodplain; if this morphological point is not known, bankfull discharge is also simply the level at which peak flow occurs about every 1.5 to 2 years (Gubernick et al., 2008). Since the relationship between vegetation and bank strength is complex, the use of remotely sensed data could be helpful for conducting large-scale studies on various natural streams and the corresponding volume of vegetation that exists on the stream bank and floodplain area. The process of quantifying the effects of riparian vegetation on streambank stability are complex in nature (Simon and Collison, 2002), but in an attempt to simplify this concept, this study aims to analyze the issue by rendering all streambank vegetation to merely values of height and volume. The objectives of this study are as follows:

1. Examine the potential impact that vegetation height and its volume has on streambank strength.
2. Calculate the coefficients that can be applied to the estimation of critical shear stress.

By using Google Earth Engine® for collecting the parameters to calculate a bank strength of a stream, as well as the existing vegetation in the floodplain. This is a low-cost and feasible way to examine bank strength based on a volume of vegetation, and these methods have the potential to be applied across larger scales. The exact methodology for calculating coefficients is explained in the next section.

2. BACKGROUND

Natural Channel Design (NCD) is an approach to stream or river restoration that aims to reduce streambank erosion by emulating the natural form of a river system (Rosgen, 2011). This approach assumes that the designer has an understanding of the stream's natural tendencies, as well as how likely it is to respond to environmental forcings. NCD uses a stream classification system that describes each stream's sedimentological, hydraulic, morphological and biological characteristics (Rosgen, 1994). The classification, however, is primarily based on the measured bankfull stage morphology of a river or stream, as the bankfull stage is responsible for shaping and maintaining the channel dimensions over time (Rosgen, 2011). Bankfull stage is typically defined at a point where the width to depth ratio is at a minimum (Fripp et al., 2001). This is also the stage at which a flooding event would occur. In the case where the actual bankfull stage cannot be measured in the field, a recurrence interval can be used to model a flood event that would fill a channel up to the bankfull stage point. Recurrence intervals are used in many applications, including NCD, city planning, and flood prediction.

NCD also looks at other factors that may impact the integrity of the stream, such as the forces acting on the stream bank. The force of water applied to the channel boundary is called the shear stress, which increases with depth and slope. Increasing the slope or water depth of the channel can increase erosion of the steam banks and stream bed. Therefore, one of the main goals of NCD is to reduce the shear stress that is exerted onto

the stream channel. The shear stress placed on the sediment particles as described by Doll et al. (n.d.) is mathematically explained by Equation 1:

$$\tau = \gamma RS \qquad \text{(Equation 1)}$$

where τ = shear stress (lb/ft^2), γ = density of water (62.4 lb/ft^3), R = hydraulic radius of the riffle cross-section at bankfull stage (ft), S = average stream slope (ft/ft). Since one of the main goals of stream restoration is to stabilize the bank and reduce erosion, knowing the strength of the streambank itself is crucial for determining if the channel's shear stress is capable of causing erosion. The critical dimensionless shear stress is a measure of the force required to mobilize and transport a given-size particle resting on the channel bed (Doll et al., n.d.). Data for this calculation are usually gathered using a bar sample and a wetted-perimeter cross-section pebble count. From that data, the median diameter of the bar sample ($d^{\wedge}_{50}$) and the median diameter of the wetted-perimeter (d_{50}) are derived. If the $d_{50}/d^{\wedge}_{50}$ ratio is between the values of 3.0 and 7.0, then the τ_c calculated using Equation 2 (Andrews 1983):

$$\tau_c = 0.0834(d_{50}/d^{\wedge}_{50})^{-0.872} \qquad \text{(Equation 2)}$$

If the $d_{50}/d^{\wedge}_{50}$ ratio is not between the values of 3.0 and 7.0, then the ratio of d_i/d_{50} is calculated, where d_i = largest particle from the bar sample. If the d_i/d_{50} ratio is between the values of 1.3 and 3.0, then the τ_c is calculated using Equation 3 (Andrews 1983):

$$\tau_c = 0.0384(d_{50}/d^{\wedge}_{50})^{-0.887} \qquad \text{(Equation 3)}$$

If the calculated critical shear stress exceeds the shear stress, then erosion should not occur. Since stream restoration planning is heavily reliant on this evaluation, it's important

that critical shear stress calculation accounts for all the factors that affect the strength of a streambank.

As mentioned in the introduction, it's been known that there is a relationship between the volume of the plant cover on the soil and the amount of soil that is lost through erosive processes (VanDersal, 1938). In natural channels, the banks are significantly rougher than the bed due to dense riparian vegetation that exist on the streambanks and floodplain (ASCE, 1998). Roots have been found to add strength to the soil by vertically anchoring the soil mass to lower substrate and by laterally binding the area together (Zeimer and Swanston, 1977). For these reinstated reasons, NCD has implemented the installation of native vegetation in its methodology to prevent or reduce stream bank erosion. Since vegetation effectively increases soil cohesion, this in turn increases the strength of the streambanks against the force of the river. Therefore the quantitative effect of planting native vegetation should be included in the calculation of critical shear stress.

Rosgen (2001) noted that a streambank erosion rate can be calculated using measurements of bank heights, angles, materials, presence of layers, rooting depth, rooting density, and percent of bank protection. This method of calculating a Bank Erosion Hazard Index (BEHI) was found to be accurate in predicting the stream erosion rates for two independent data sets (the West Fork Madison River, Montana and the East Fork River, Colorado). However, the direct influence of vegetation on stream bank strength is not quantified. Furthermore, if stream restoration planners are using a critical shear stress equation to estimate the potential erosion for a given stream, it should not be solely based on particle size.

In order to attempt to quantify the general effect that vegetation has on the critical shear stress of a streambank, a few studies have formulated methods to assess a stream's critical shear stress by way of its channel geometry. Huang and Warner (1995) laid the framework for determining the specific factors that affect the shape of a channel. While the concept of hydraulic geometry in alluvial channels was first described by Leopold and Maddock (1953), Huang and Warner (1995) developed a multivariate model of channel geometry that explains the relationship between channel shape and boundary shear distribution. The general form of river channel geometry, as proposed by Huang and Warner (1995) is described in Equations 4-6:

$$W = C_W Q^{0.5} n^{0.355} S^{-0.156} \qquad \text{(Equation 4)}$$

$$D = C_D Q^{0.3} n^{0.383} S^{-0.206} \qquad \text{(Equation 5)}$$

$$A = C_A Q^{0.8} n^{0.738} S^{-0.362} \qquad \text{(Equation 6)}$$

where W represents channel width, D represents depth, A represents cross-sectional area, Q represents flow discharge, n represents channel average roughness, and S represents slope. C_W, C_D and C_A are generally variable and, as analyzed by Huang and Warner (1995), they physically relate to the critical shear force τ_{cbk} for the movement of bank material (Equations 7 - 9) as follows:

$$C_w \alpha \tau_{cbk}^{(-5J)/(8-5J)} \qquad \text{(Equation 7)}$$

$$C_D \alpha \tau_{cbk}^{(-5J)/(8-5J)} \qquad \text{(Equation 8)}$$

$$C_A \alpha \tau_{cbk}^{(-5J)/(8-5J)} \qquad \text{(Equation 9)}$$

C_W was determined to be the coefficient most responsive to bank strength. According to Huang and Warner (1995), J in Equations 7-9 is a constant between 0.25 and 0.35.

Huang and Nanson (1998) further demonstrated that both bank sediment and bank vegetation play an important role in influencing the alluvial channel width and depth. This study further gathered field data from gravel-bed rivers in the UK, USA, and Australia and divided the site locations into categories of four quantitative types of vegetative cover: grass, 1-5% tree/shrub, 5-50% tree/shrub, >50% tree/shrub. The C_W, C_D, and C_A for each site were calculated as well. Densely vegetated banks (> 50% tree/shrub cover in gravel rivers in the UK) were found to exhibit the smallest values of C_W, and were therefore stronger at resisting erosion.

Julien and Torres (2005) aimed to identify the controls on erosion of riverbanks in the Sand River in Aiken, SC. The researchers calculated the critical shear stress τ_c by using a silt-clay percentage in conjunction with vegetation coefficients that were derived using data from Huang and Nanson (1998). The calculated coefficient increased as areal coverage increased (none 0%, Sparse <25%, medium 25-75%, dense >75%) from 1 to 1.5 to 2 to 2.5, respectively. To calculate the coefficients, Julien and Torres (2005) used the C_W from the Huang and Nanson (1998) datasets to calculate the τ_{cbk} using Eq. 7. After τ_{cbk} values were calculated, they divided each τ_{cbk} value by the lowest value in the dataset to calculate a factor. The factor represents how much the critical shear stress value is increased by the presence of vegetation. The factor for dense trees in the Australia dataset from Huang and Nanson (1998) was divided by the factor in the UK dataset from Huang and Nanson (1998), as was similarly done for sparse trees. Those values were averaged and multiplied by the factor values in the UK dataset to produce an overall value for the UK dataset. From these two datasets, average values for each vegetation type were

calculated. The resulting coefficients of 1, 1.97, 5.4, and 19.7 were calculated for non-vegetated, grassy, sparse trees, and dense trees respectively.

The purpose of detailing the findings of Julien and Torres (2005) is to show that the quantitative effect of vegetation on critical shear stress has been quantified. Therefore, this study aims to continue this methodology, but with a numerical categorization of bank vegetation, in the form of a vegetation volume, that can be applied to streams in Texas or hydrologically and geologically similar areas.

As stated earlier, vegetation has a significant influential role on channel geometry. Densely vegetated banks have been shown to increase bank stability by increasing soil cohesion through the vegetation's root structure, and this increased bank stability is generally associated with less widening of the stream or river channel (Huang and Nanson, 1997). Jang and Shimizu (2007) found that as vegetation density increases in the bed and banks, the bank erosion rate is reduced. Dense vegetation is also associated with an increase in channel depth and flow resistance (Hickin, 1984). Therefore, the slope of the channel bank could lend insight on the status of the bank's strength and stability. Thus, the slopes of each station location's stream bank will be assessed to see if there is an influence or correlation between stream bank slope and percent volume of vegetation (PVV).

Given that bank strength can be indirectly calculated if all the parameters are known in Equations 4-9, this study aims to compare the calculated bank strengths of various streams in Texas with the associated vegetative cover. In addition to providing a PVV that corresponds with a general index of bank strength, this study aims to better

understand the relationship between bank slope on bank strength, as well as the role of lithology and soil type in comparing the relationship between bank strength and PVV.

2.1. Study Area

Fig 3. provides a detailed view of all the stations that are included in this study. All stations are in southeast to south central Texas. Nearby major cities include Houston, Austin, and San Antonio. The dominant lithology in the area is sand, followed by clay or mud. In this study, a series of stream profiles and discharge data were collected at various USGS stations. The bank strengths were calculated at each station along with the percent volume of vegetation (PVV), and these values were compared amongst each other, separated according to the dominant lithology of the station area, as well as by hydrologic soil group.

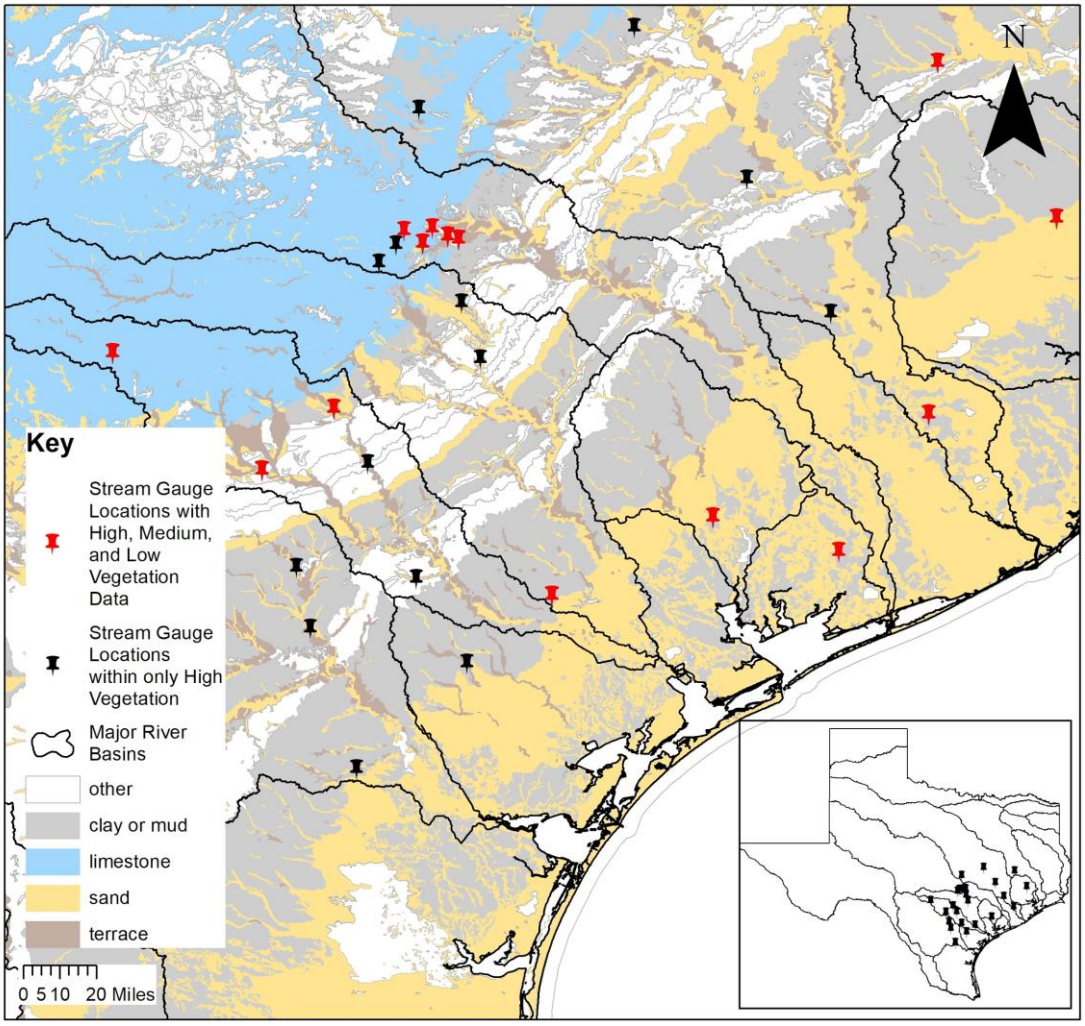

Figure 3. Spatial distribution of the stations included in this study. The station points in red show stations that have Lidar data for medium and low classified vegetation, in addition to high vegetation. The points in black only have lidar data for high vegetation

Be sure that the Title Page has no page number, the preliminary pages have lowercase roman numeral page numbers beginning with Abstract on p. ii, and that Section 1 begins on p. 1.

3. METHODS AND MATERIALS

3.1. Data Stations

This study focuses solely on USGS-gauged streams within Texas. A point shapefile of all USGS stream gauge stations was downloaded from https://water.usgs.gov/. This shapefile was imported into Google Earth Engine®, along with shapefiles delineating river basins, geologic layers and features, and Lidar Point Cloud (LPC) and Digital Elevation Model (DEM) availability. A shapefile of the geologic layers and features for the state of Texas was accessed from the USGS website. The lithology at the surface of each stream location was extracted from the USGS shapefile, representing the dominant rock types according to the regional geology. The stations in this study fell on the following USGS lithological categories: clay or mud, sand, limestone, and terrace. A terrace is defined by the USGS as a landform that forms when streams carve downward into their floodplains, leaving discontinuous remnants of older floodplain surfaces as step-like benches along the sides of the valley. Terraces preserve or display unique characteristic soil profiles or weathering characteristics because of their long-standing isolation from stream erosion. Soil data were also downloaded from the Web Soil Survey, an online soil database, which is a product available through the Natural Resources Conservation Service, USDA.

Only stations that had available LPC and DEM data were kept for analysis. Some stations had LPC data that only showed the top-of-canopy heights of vegetation in the

area, while others provided vegetation heights for medium and low-lying vegetation as well. All bayous and canals were excluded from the selected stations.

3.2. Modeling Bankfull Discharge

Bankfull stage or depth is the highest point of a river or stream that can be contained within the channel without spilling water onto the floodplain (Fig. 1), and it is also reported to occur every 1.5 to 2 years (Rosgen, 1996). Due to the data available, the latter definition is used in this study. The USGS provides current and historical gauge height with each corresponding discharge value. From the selected USGS stream gauge stations, peak streamflow data were gathered for each station from the USGS National Water Information System. Stations that had less than 10 years of data were removed from the list of selected stations. Historical peak streamflow data from the USGS were used to calculate the bankfull discharge that would occur for a 1.5 year flood. The exceedance probability of a 1.5 year flood is equivalent to the flood discharge that would occur for 83.33% and 66.67% of the peak flow discharges, respectively. Bankfull discharges and depths for each station are shown in Table 6 in the Appendix.

An alternative method for obtaining a station's bankfull discharge would be to collect the stream profile at the USGS station, and then assess where the natural indicators of bankfull, as outlined in McCandless and Everett (2002). Once the bankfull depth is known from the stream profile, it could be compared to the USGS station-specific depths provided for peak streamflows to determine the corresponding bankfull discharge associated with that depth. However, the recurrence interval for bankfull discharge

associated with the dominant indicators range from 1.05-1.8 years, and the manually-inferred bankfull depth may not fall within this range. To avoid this situation, the aforementioned method was used. Furthermore, it is a well-accepted tenet (Gubernick et al., 2008) that bankfull discharge occurs at approximately the 1.5 year recurrence interval, and for that reason, this study chose to use the associated depth and discharge for a 1.5 year flood. A broader overview of this process, and the entirety of all the methods in this study can be visualized in Fig. 4.

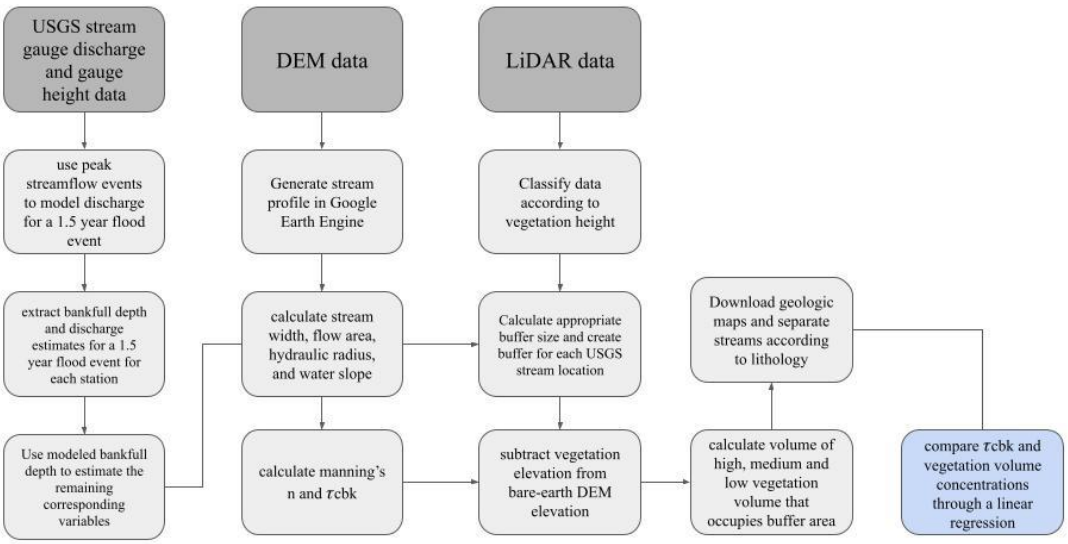

Figure 4. Overview of the workflow for this study.

3.3. Stream Profiles

To generate a stream profile, a digital elevation model (DEM) for each station location was imported into Google Earth Engine®. Each pixel value corresponded to a 1x1 meter square area. Latitudes and longitudes were attached to each pixel in the DEM,

and a function was created to extract all the elevations at each pixel that intersects with the transect line to generate a stream profile at any drawn line across the stream bank. Transects were delineated to lie perpendicular to the stream centerline, while also intersecting the USGS stream gage location point from the downloaded shapefile. Examples of a generated stream profile is shown in Appendix A.

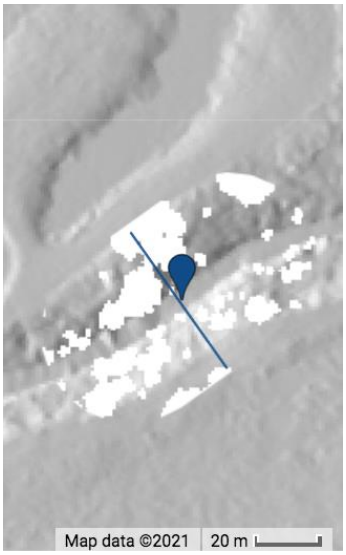

Figure 5. Stream profile of USGS station 08162600 and the bird's eye view of the buffer area at USGS station 08162600, with the transect line shown in blue. The blue point represents where the stream gauge sensor is. At this station, the modeled bankfull depth was calculated to be 3.73015 meters, and that number was used to gather the bankfull width, cross-sectional area, and wetted perimeter.

The remotely sensed stream profiles were ground-truthed using in-situ profile measurements. Slopes along each bank were also calculated using the generated stream profiles. This was done by extracting the elevation at the left side of the profile at bankfull height and at the lowest elevation on the leftmost side, and dividing the difference by the

horizontal distance between the two points. The same process was done on the right side of the bank.

3.4. Calculating Bank Strength

After modeling bankfull discharge at each station using the provided discharge, the corresponding gauge height measurement was used to determine the bankfull elevation on each stream profile. As described earlier, if the calculated bankfull depth from a 1.5 year flood for the station could not be obtained from the profile due to the height exceeding the natural height of the profile, the station was omitted from the selected stations. The bankfull area was calculated using a Reimann sums approach from the generated stream profile. The wetted perimeter was calculated using Eq. 10. Bank strength was calculated using the equations in 4-9. The calculations of bank strength are an indication of how stable each bank is.

$$P_{wetted} = b + 2y\,(1+z^2)^{0.5} \qquad \text{(Equation 10)}$$

$$Q = (1/n)\,AR^{2/3}(S)^{0.5} \qquad \text{(Equation 11)}$$

where b = basal width of the profile, y = height or depth, and z = slope of the sides of the profile. After determining the bankfull depth, basal width, bankfull width, and cross-sectional area, the hydraulic radius was calculated by dividing the cross-sectional area by the wetted perimeter. Manning's n was back-calculated using Manning's Equation (eq. 11), and according to Rosgen (2007), Manning's n can be back-calculated if velocity, slope, and hydraulic radius are known; the bankfull discharge used in this calculation was the modeled bankfull discharge from the 1.5 year flood. To calculate the water surface

slope of the area, a line was drawn 500 meters upstream and 500 meters downstream from the stream profile, ensuring to follow the stream's meander. A line was drawn at both ends of the stream line, and the minimum elevation was extracted from each line. The difference between the minimum elevations was calculated and then divided by the full length of the stream line to calculate the slope. The process is visualized in Fig. 6.

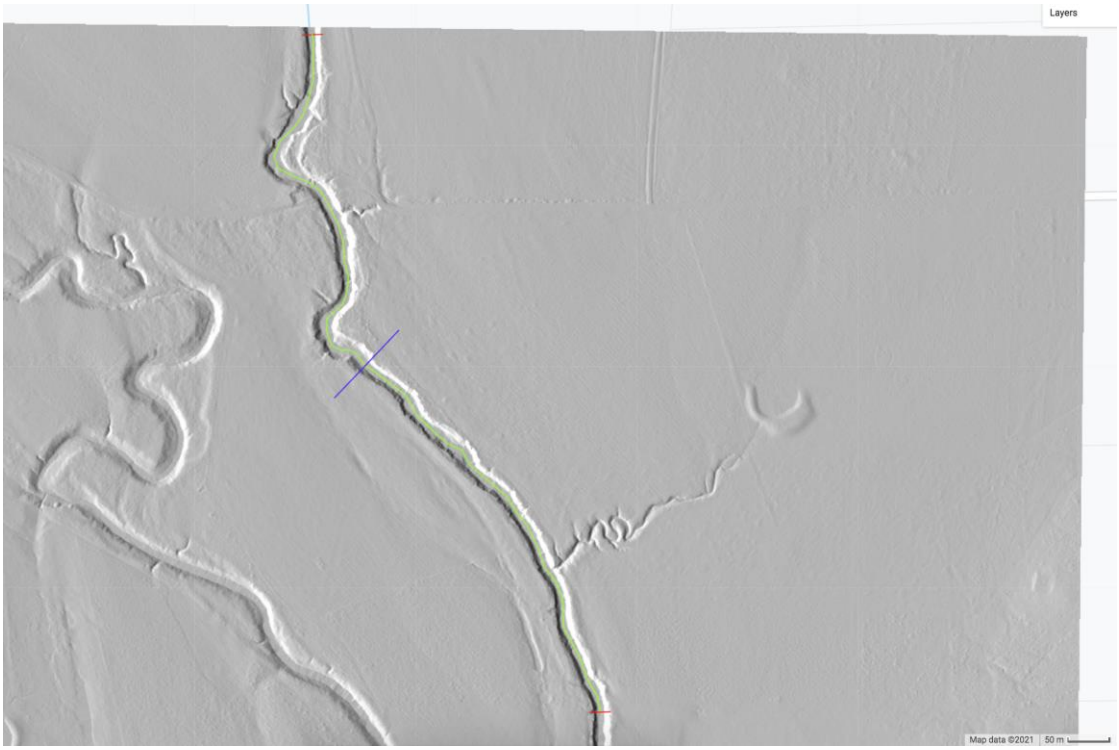

Figure 6. Visualization of the slope calculation process. The line in purple shows where a stream profile was taken, the green line is the length of the line used to calculate the horizontal distance of the slope. The binding lines in red were used to estimate the lowest elevation or the bottom of the stream profile at that location. Differences between these minimum elevations were calculated and divided by the length of the horizontal distance shown in green.

Using the values obtained from the stream profile and the discharge provided by the USGS, the final calculation of τ_{cbk}, or bank strength, was calculated using Equation 7.

3.5. Calculating Vegetation Volume

To create a buffer that would collect all the vegetation within it, a line bisecting the stream (lime green line in Fig. 6) was drawn along each stream location, approximately 30 meters upstream and downstream from each USGS stream gauge location. Tree root systems extend out about 1.5 times the height of the tree (Day and Wiseman, 2009), and since the maximum height of the tallest vegetation out of all the station areas was roughly 20 meters, a buffer radius of 30 meters was chosen to fully account for the effect that the root system would have on the stream bank strength at each station location. To account for wider streams, in which the channel or non-vegetated area may take up a large portion of the buffer area, a larger buffer was used; if the width of the stream exceeded 45 meters, the buffer radius was calculated as (bankfull width / 2) + 5 meters. All streams with widths under 45 meters had a standard buffer radius of 28 meters. Each LPC was clipped to each station's buffer area. An LPC is a point cloud that was created using Lidar. Lidar stands for LIght Detection and Ranging, and it's a form of remote sensing that uses a laser light sensor to measure the travel time from the instrument to the target. Lidar is useful because it provides information about elevation, and in this case, vegetation height. The USGS processed the LPC data to only pick up the heights of vegetation, rather than mistakenly picking up the heights of other man-made structures such as houses or telephone poles. In Fig. 7, an LPC is overlaid on top of the imagery to show how the LPC only picks up vegetation.

Figure 7 Image showing the accuracy of how the LPC dedicates land area as vegetation. The transparent light gray overlay represents the vegetated area. The line in blue shows where the buffer line was drawn for this station location.

Using Google Earth Engine®, each pixel elevation value in the bare-earth DEM was subtracted from each pixel elevation value in the clipped LPC. In order to calculate a vegetation volume, an initial volume was created by multiplying the area of the buffer by 40 meters, a height that exceeds any top of vegetation, shown in Fig. 8.

Figure 8. Visual of the process used to extract the volume of vegetation on a streambank. The sum of all the heights of each 1x1 meter vegetation pixel (high, medium, and low) are multiplied by the area of the buffer to get a volume of vegetation. This volume is then divided by the total volume of the initial volume (bank area x 40 m) to get a percent volume of vegetation.

The sum of all the elevation differences collected in the buffer area was divided by the initial volume to calculate a PVV, or the percent vegetation volume that takes up the space of the initial volume. The USGS provides Lidar data that collects the height of the top-most vegetation, but it also collects the height of all medium-lying and low-lying vegetation in some locations. A separation of the heights found in this study are shown in Table. 1.

Table 1. Maximum and mean vegetation heights within the buffer area at all the stations that had vegetation classified as either "high", "medium", or "low." Classifications follow vegetation height category labels established by the USGS.

	Maximum	**Mean**
High	20.2	12.3
Medium	5.9	2.5
Low	2.5	0.7

Some stations lacked Lidar data that provided separate vegetation classes, but wherever possible, the vegetation density was calculated for medium and low-lying vegetation, in addition to high vegetation. A visualization of the spatial distribution of low, medium, and high vegetation is shown in Fig. 9. For a cross-sectional view of the distribution of the vegetation, see Fig. 10.

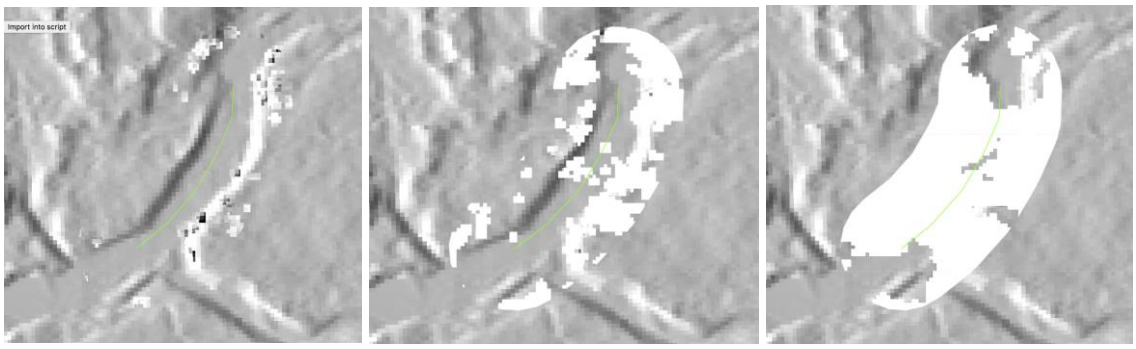

low medium high

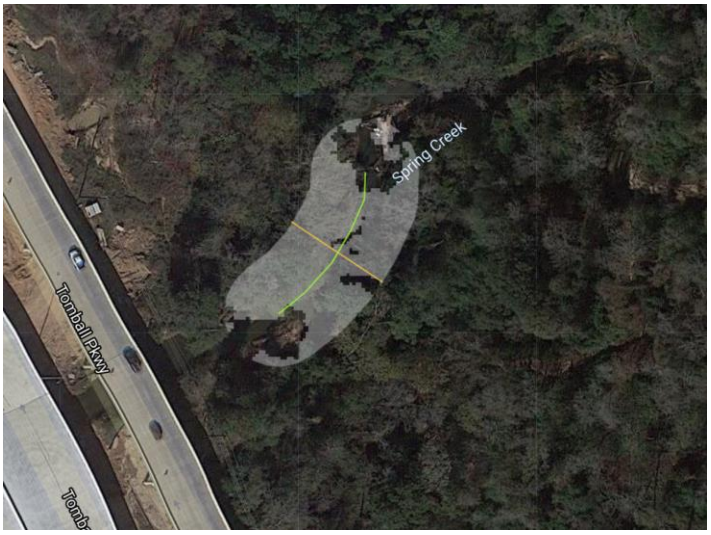

Figure 9. Visualization of how the vegetation is gathered using the buffer system. The USGS station point lies directly on the yellow transect, which is where the stream profile was gathered. The radius of the buffer shown here is 28 meters, while extending laterally about 30 meters on each side of the transect.

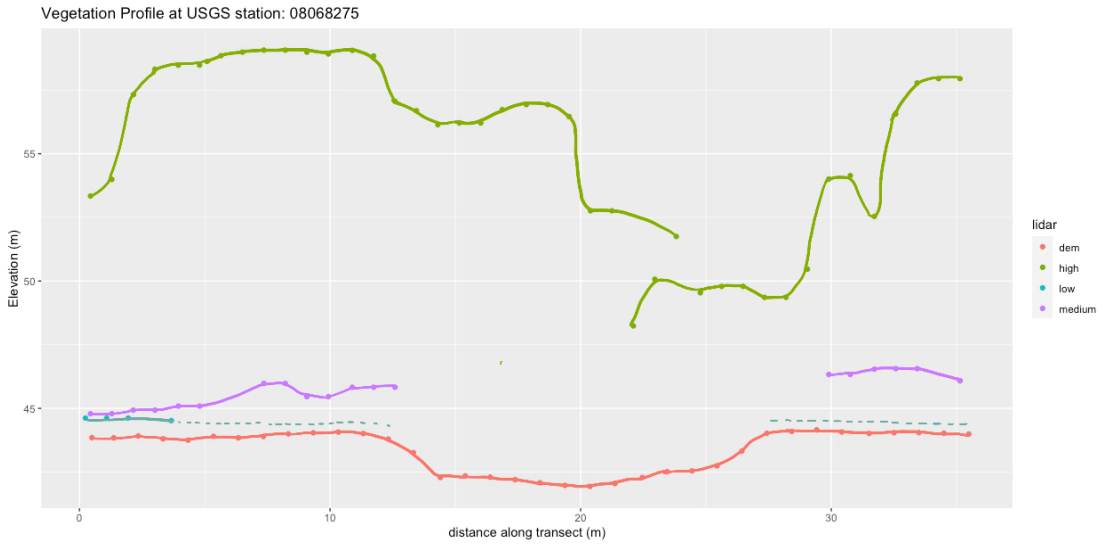

Figure 10. Cross-sectional view of the vegetation as it exists at USGS stream location 08068275. The orange line shows the stream profile, while the green, purple, and teal lines show the different classes of vegetation and how they plot along the profile. The green line representing the high vegetation shows how the LPC is able to pick up the full extent of the canopy as it hovers over the channel. This profile is for visualization purposes only. This station's vegetation was re-run to encompass a lateral distance of 60 meters.

In order to estimate vegetative cover using LiDAR data, Griffin (2006) quantified the data as a percent canopy cover, or percentage of area that is covered by pixels classified as vegetation. Percent canopy cover is important in forestry practices to predict fire behavior, air quality, and carbon sequestration amounts (Coulston et al., 2012). However, since this study is looking at low, medium, and high vegetation cover, a percent canopy cover does not include the influence of medium and low vegetation, and therefore, a percent vegetation volume is used in its place.

3.6. Statistical Analysis

A linear regression analysis was performed within each lithological group of stations to evaluate the relationship between bank strength and PVV (tall, medium, and low vegetation). Each model was separated according to the stream's geological substrate (i.e. limestone, clay or mud, sand, terrace) as well as by hydrologic soil group (i.e. A, B, C, C/D, D).

The t-test demonstrates the reliability of these differences, or whether they are a product of chance. The study adopted p-values of 0.05 or 0.10, as appropriate, to determine significance. The rule of thumb is that a study needs 10 data points in order to compare variables through a linear regression, however, given the nature of this study and the lack of lidar coverage in many streams, the amount of data points was sufficient to conduct this method of analysis.

3.7. Tree Count

A tree count was conducted within the generated buffer area at station 08158970 at Williamson Creek to provide a tangible reference for the amount of trees that could be expected given a volume of high vegetation. Pictures were taken with a human, Ben Grunau, for scale. His height is 1.77 meters. The circumference of a representative small, medium, and large tree was taken at breast height.

Figure 11. These three panels show the representative trees from station 08158970. Small, medium, and large trees are shown from left to right. In the leftmost picture, the student is collecting the tree's circumference. Photos were taken in March 2021.

3.8. Assumptions

- The DEM-generated stream profile collected at the USGS station is representative of the stream's general geometry. In order to make future applications of this

technique more robust, multiple stream profiles should be taken along the buffer area, and the average measurements should be used.

- The LPC is representative of the current vegetation in place, regardless of natural variations that may occur due to seasons.
- The DEM-generated stream profile is representative of the stream's current geometry and physical attributes.
- The streams used in this study have not been realigned or altered to minimize or increase erosion.

4. RESULTS

After applying a series of filters, a total of 25 stations were selected for this study. Out of those stations, only 14 had separate classifications for vegetation (i.e. low, medium, and high), and therefore, only those were used in the analysis between low to medium vegetation and bank strength. The selected USGS stations fell within the Brazos, Colorado, Guadalupe, Lavaca, Nueces, San Jacinto, Trinity, and San Antonio River Basins (Fig. 3). Each station's bank strength (τ_{cbk}) and PVV (low, medium, and high) were plotted and separated according to the dominant lithology that corresponds to that station location. To check for outliers, bank strengths at each station were plotted in a box plot to identify any data points outside the 1.5 interquartile-range for each lithological category. For the sand streams, stations 08111700 and 08172400 were removed. After removing outliers, the resulting relationship between bank strength and PVV is shown in Fig. 12, Fig. 13, and Fig. 14. The box plot depicting the outliers that were removed is shown in Fig. 45 in the Appendix.

Results from the linear regression analysis are shown in Table 2. Qualitatively, bank strength is shown to increase with increasing PVV for high vegetation in sand, terrace, and clay or mud streams (Fig. 12). There appears to be no influence of PVV on limestone streams. Bank strength decreased with increasing PVV for medium vegetation in sand and clay or mud streams; however, it increased in terrace streams, with little to no change in limestone streams. The same observation can be seen with PVV for low vegetation. There was a statistically significant relationship ($p<0.05$, $R^2 = 0.5877$) between bank strength and high vegetation within stations located on clay or mud-dominated

lithologies. There was also a statistically significant, albeit less strong relationship ($p<0.1$, $R^2 = 0.8723$) between bank strength and high PVV within stations located on sand-dominated lithologies. Given the nature of this research, a p-value less than 0.1 is sufficient enough. Within the stations with low vegetation, there was a statistically significant relationship between bank strength and PVV for sand streams ($p<0.05$, $R^2 = 0.8723$).

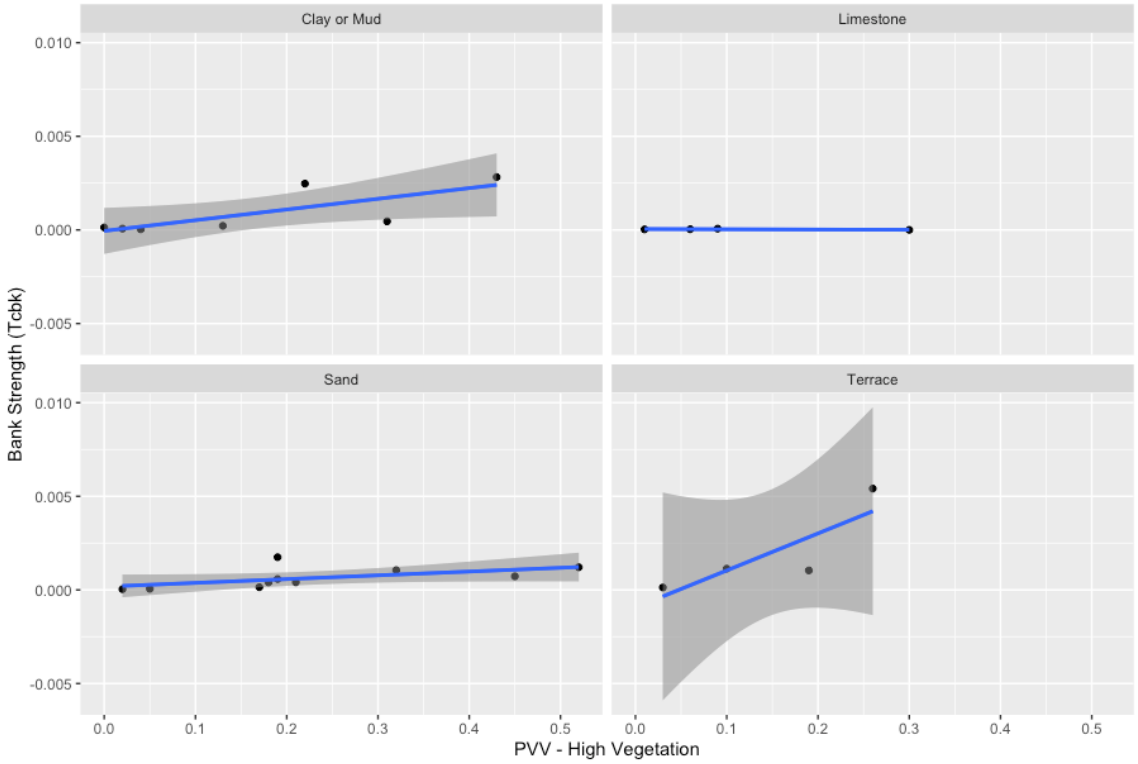

Figure 12. Distribution of PVV for high vegetation and the corresponding bank strengths at each station. Outliers were removed. Also, there are more data points in the high vegetation because the medium and low PVVs could not be obtained at some stations due to complications with downloading the data. Best fit lines are separated according to the associated geologic characterization.

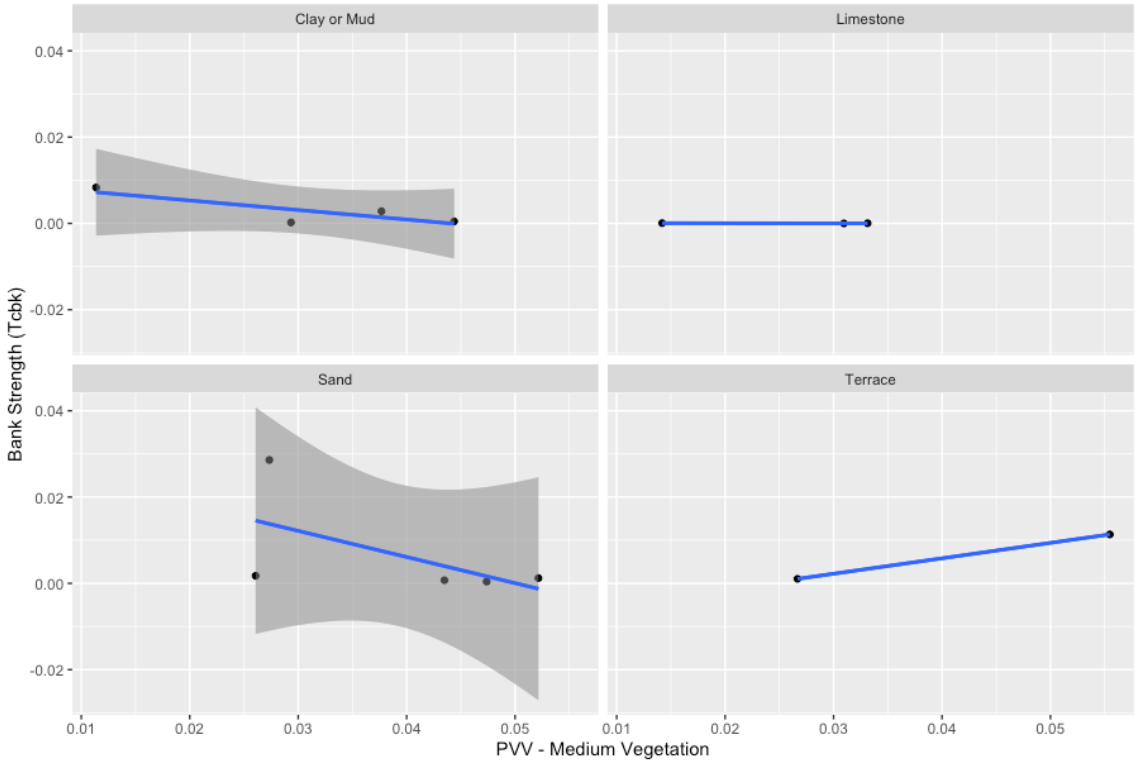

Figure 13. Distribution of percent volume of vegetation for medium vegetation and the corresponding bank strengths at each station. Best fit lines are separated according to the associated geologic characterization.

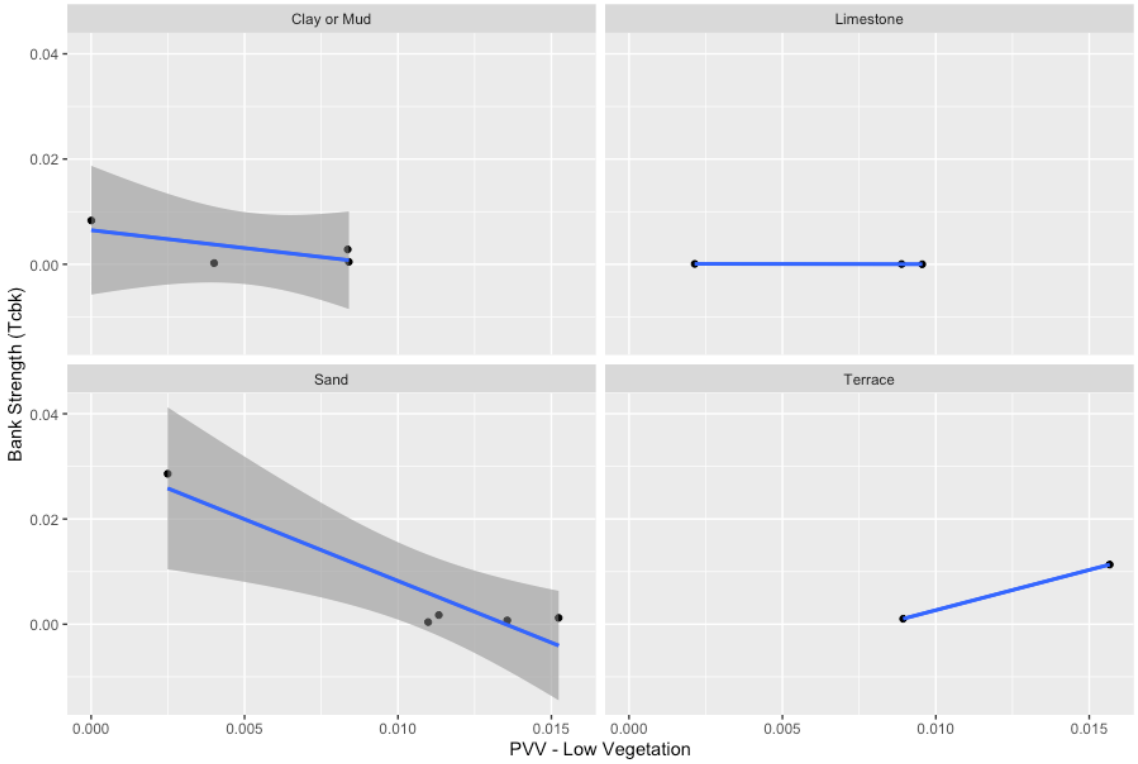

Figure 14. Distribution of the PVV for low vegetation and the corresponding bank strengths at each station. Best fit lines are separated according to the associated geologic characterization.

Table 2. Results of the linear regression analysis within stations grouped by lithology. Within the stations located on a clay or mud-dominated lithology, there is a statistically significant relationship between bank strength and high PVV ($p < 0.05$). Within the stations located on a sand-dominated lithology, there is also a less statistically significant relationship ($p < 0.1$) between bank strength and high PVV.

bank strength and **high** PVV

lithology	Std. Error	t value	p-value	multiple R-squared
clay or mud	0.00214	2.67	0.0444	0.587
limestone	0.000114	-1.16	0.366	0.402
sand	0.001	1.98	0.082	0.330
terrace	0.00892	2.215	0.157	0.710

bank strength and **medium** PVV

lithology	Std. Error	t value	p-value	multiple R-squared
clay or mud	0.454	-1.494	0.274	0.5273
limestone	0.003	-1.88	0.311	0.779
sand	0.518	-4.52	0.020	0.872
terrace	NA	NA	NA	NA

bank strength and **low** PVV

lithology	Std. Error	t value	p-value	multiple R-squared
clay or mud	0.454	-1.49	0.274	0.527
limestone	0.003	-1.88	0.311	0.779
sand	0.518	-4.52	0.020	0.872
terrace	NA	NA	NA	NA

Station data were also separated according to the hydrologic soil group based on NRCS soil maps; results are shown in Table 3. Stations located on soil classified as hydrologic soil group A showed a moderately statistically significant relationship between bank strength and PVV for low vegetation ($p<0.1$, $R^2 = 0.2491$). The distribution between bank strengths and hydrologic soil group can be found in Fig. 46 in the appendix.

Table 3. Results of the linear regression analysis within stations grouped by hydrologic soil group. Within the stations located on an A-classified hydrologic soil group, there is a statistically significant relationship between bank strength and low PVV.

bank strength and **high** PVV

Hydrologic soil group	Std. Error	t value	p-value	multiple R-squared
A	0.025	0.232	0.824	0.008
B-D	NA	NA	NA	NA

bank strength and **medium** PVV

Hydrologic soil group	Std. Error	t value	p-value	multiple R-squared
A	0.026	0.232	0.824	0.008
B-D	NA	NA	NA	NA

bank strength and **low** PVV

Hydrologic soil group	Std. Error	t value	p-value	multiple R-squared
A	0.005	2.06	0.084	0.249
B-D	NA	NA	NA	NA

Stream bank slopes on both the right and left side of the profile were plotted in Fig. 15. according to lithology. There was no clear consistency between both the left and right bank slope and lithology, aside from clay or mud streams having relatively similar slopes on both their right and left banks. After conducting a linear regression on the relationship between left bank slope and bank strength in clay streams, the two variables were shown to be statistically significant (p-value = 0.0119, $R^2 = 0.8271$). The right bank slope, however, did not show any statistically significant relationship (p-value = 0.168, $R^2 = 0.4138$). There was no significant relationship observed between the bank slope within the other lithological groups.

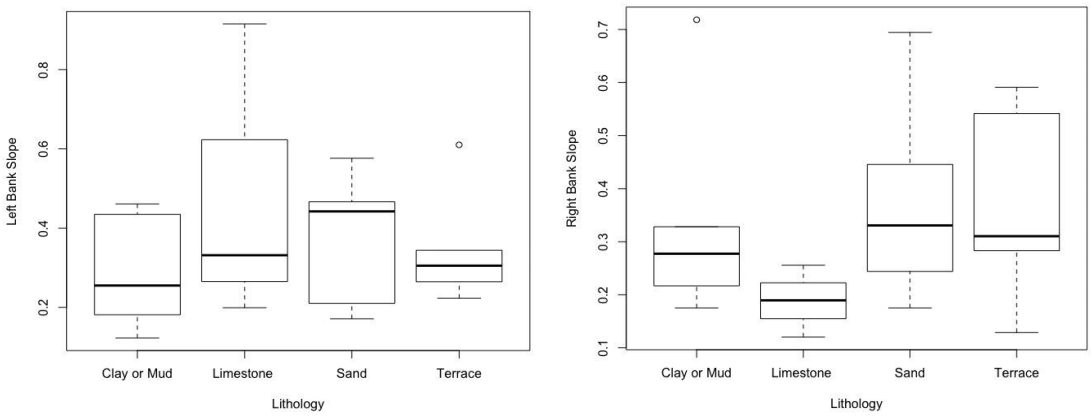

Figure 15. Box plots of the left and right bank slopes along the stream bank profiles.

The following plots show a visual relationship between the field collected stream profiles and the Google Earth Engine ® generated profiles:

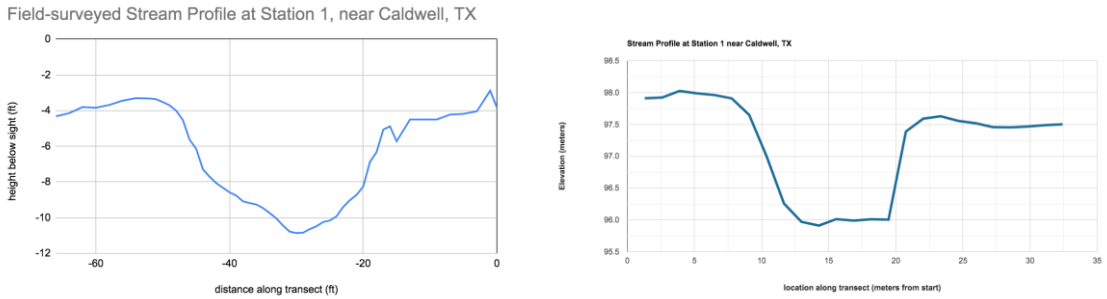

Figure 16. Visualization of a field-collected stream profiles (right) and the corresponding Google Earth Engine ® generated stream profile (left). Two other field-collected stream profiles were gathered and are shown in Appendix A.

A table containing width and depth measurements for 3 stream profiles are shown in Table 7 in the appendix. The Google Earth Engine® generated profile and the field-collected profile differed in depth from 2.57% - 12.22%, and the width measurements differed by 22.57 - 35.34%.

The vegetation and bank strength data from the sand and the clay or mud streams was used to calculate critical shear stress coefficients that can be applied to a critical shear stress equation (eq. 2 and eq. 3). The τ_{factor} was calculated by dividing the τ_{cbk} values by the lowest value in each lithological group. An explanation of the process of calculating critical shear stress coefficients is outlined in Julien (2004). The results from this study are shown in Table 8 in the Appendix. A coefficient of 1, 14.6, 15.4, and 20.0 corresponds to 0%, 20%, 30%, and 40% PVV for high vegetation respectively. The percentages of vegetation and corresponding coefficients are shown in Fig. 17. After plotting the PVV for high vegetation with each corresponding coefficient, a relationship was deduced between the two variables (eq. 12).

$$c = 46.2\ p + 2.28 \qquad \text{(equation 12)}$$

where c is the coefficient that can be applied to an existing equation for critical shear stress and p is the percent volume of vegetation.

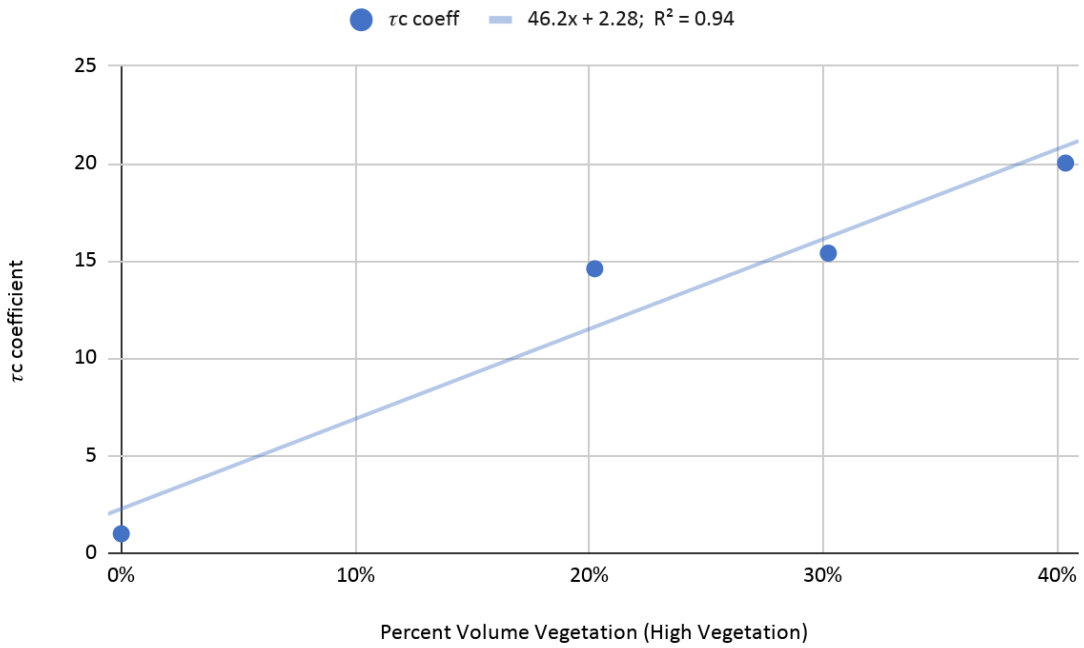

Figure 17. Plot of PVV for high vegetation and the corresponding coefficient that can be applied to a critical shear stress equation. As shown, a bank area with a PVV of 40% is assumed to have roughly 20 times the critical shear stress as if that area were to have roughly 20 times the critical shear stress as if that area were to have no high vegetation.

After conducting a tree count within the buffer generated at station 08158970, a total of 53 small trees, 26 medium trees, and 19 large trees were counted. This station's volume of high vegetation was calculated to be 45.74%, therefore for a similar volume of vegetation in the Austin area, a similar tree count can be expected to exist on the streambank within the buffer area. The circumferences of relatively small, medium, and large trees can be found in table 4.

Table 4. Tree counts and circumference measurements for a representative small, medium, and large tree in the buffer area.

	small	medium	large
right bank	13	13	18
left bank	40	13	1
total	53	26	19

circumference	0.48 meters	1.19 meters	2.46 meters

5. DISCUSSION

5.1. Bank Slope

Stream bank slope can be an indication of the threshold of vegetation that is needed to stabilize a stream bank (Krzeminska et al., 2018). The left and right bank slopes of the 23 stream profiles varied greatly within and between streams. There is a correlation between left bank slope and bank strength in clay streams (p-value = 0.01193, R^2 = 0.8271). This result could be due to the taller vegetation generally having deeper roots that allow steeper slopes to exist (Pollen-Bankhead and Simon, 2010). There was no significant correlation between right bank slope and bank strength (p-value = 0.168, R^2 = 0.4138). It is unclear as to why there was so much variation between the left and right bank slopes. The relationship is not as strong, however as compared to the effect that PVV had on bank strength.

5.2. Soil Type

There was no statistically significant relationship between soil type and bank strength. The average bankfull depth of the stream profiles was 3.19 meters, and since most of the soil survey data does not provide soil profiles that go deeper than 1.5 meters, this could explain why there was no discernable relationship between soil type and bank strength. Soils with a higher water content tend to have less stability (Wang and Cong 2019). Since Groups A and B soils have low to moderately low runoff potential, meaning that the soil moisture is likely greater than in soil groups C and D, Groups A and B soils

were hypothesized to have lower overall bank strengths; however, the box plot shown in Fig. 46 of the Appendix does not clearly show lower bank strength values for Groups A and B, but soil group D has the highest upper quartile values of bank strength. More data are needed to analyze the relationship between bank strength and soil type.

5.3. Geology

Interestingly, the geologic substrate of each station had a significant influence in determining where this method of evaluation has the most significance. In limestone streams, it is clear that no matter the PVV, bank strength does not change in response, according to this small sample size. The reason there was little to no change in bank strength, despite an increase in PVV, could be due to the effect it has on soil aggregation. Cerda (1996) noted that vegetation is less important than lithology in influencing soil aggregate stability. In that study, three Mediterranean landscapes in southeast Spain were analyzed; the lithological influence on aggregate stability was found to be higher than the influence from the vegetation cover. In clay or mud, sand, and terrace streams, the opposite was true; vegetation had a noticeable effect on streambank strength, with results varying according to the classification of vegetation height.

5.4. Vegetation Height

In sand, clay or mud streams, bank strength was found to increase with increasing PVV for high vegetation. Also, an increasing PVV of medium and low vegetation cover was shown to generally decrease the bank strength in terrace, clay or mud, and sand

streams; however, these latter results are less compelling because there were far fewer data points for low and medium vegetation when compared to the high vegetation. Also, since the PVV is a percent volume out of a total volume that is 40 meters in height, the impact of the low and medium vegetation was less discernible since the low vegetation averaged less than 1 meter in height, and the medium vegetation averaged 2.5 meters in height. Future work should focus on assessing the impact of low and medium vegetation, with a buffer height that better reflects the impact of that type of vegetation.

Since high vegetation was associated with high bank strength, and low was and medium vegetation was associated with lower bank strength, this could be explained by the results found in Krzeminska et al. (2018), where streambanks on marine clay soils were covered with different types of vegetation typical of Norwegian agricultural areas. There were no differences in stream bank stability between the grass and shrub plots, but there was significantly lower soil moisture content, soil porosity, and higher shear strength within the tree plot. The area with trees was the most stable and showed the highest capacity to accommodate potential shear stress. In their conclusions, they found that slope angle dictated the type of vegetation that was necessary to sufficiently reinforce the stream bank. For gentle slope angles, grass cover is sufficient, but tree cover is necessary to protect steeper slopes against slope failures. It appears that the bank strength values were more responsive to the presence of high trees, leading the researchers of this study to conclude that this methodology is better suited for analyzing the effects of high trees on bank strength. Another potential explanation for this could be that since the area is being occupied by low or medium vegetation, it is taking space that could otherwise be occupied

by high vegetation. Since the presence of high vegetation typically represents a deeper and wider root extent, this could explain the increase in bank strength with increasing PVV for high vegetation. Also, the presence of high vegetation could yield a decrease in lower lying vegetation because a widespread canopy cover prevents the infiltration of light needed to grow lower-lying vegetation. Therefore, the lower PVVs for medium and low vegetation associated with relatively higher bank strengths could be a function of the streambank area not being hospitable for lower-lying vegetation. It's also worth noting that the decreased sample size for medium and low vegetation makes it harder to determine the relationship between PVV and bank strength. In order to better understand this relationship, more data points should be added in future work.

5.5. Profile Accuracy

While the accuracy between the Google Earth Engine ® generated stream profile and the field-collected stream profile is not high, this approach will improve with time. As the reliability and spatial resolution of LiDAR and DEM data improve, it is expected that discrepancies between in-situ derived stream profiles will be bolstered. Furthermore, the increasing initiative for open-source data, and free access to cloud-based remote sensing and geospatial platforms such as Google Earth Engine, dramatically increases user friendliness and allows similar studies to be readily conducted at low-cost by a wider range of users. Foremost, this approach saves users time that would otherwise be used to manually collect stream profiles, greatly enhancing the spatial coverage over-which these types of studies can be conducted.

5.6. Future Work

The next step in this project would be to ground truth all the observations made in this study, as well as perform a vegetation assessment for each station location to determine the plant species present at each location in order to further clarify the role of root system effect on bank strength. Additionally, more data points are needed from low and medium vegetated areas to better assess the influence of this type of vegetation on bank strength.

6. CONCLUSION

The results of this study indicate that there is a statistically significant relationship between PVV for high vegetation and bank strength in sand, clay, or mud streams, meaning that the higher the PVV for high vegetation, the more stable the streambank will be. Since the root extent of high vegetation is relatively deeper and wider than that of low and medium vegetation, it could be concluded that the higher bank strength is attributed to the deeper and more widespread root system imposed by high vegetation. Also, there was an overall decrease in bank strength associated with increasing low and medium PVVs in sand and clay or mud streams; however, more analysis is needed to better evaluate this relationship. Regarding limestone streams, there was no influence of PVV on bank strength in either of the vegetation height classes, indicating that bank stability in limestone streams has more to do with particle aggregation than with the addition of vegetation. Overall, this helps elucidate the effect that PVV may have on streambank stability, when comparing low, medium, and high vegetation in Texas streams. Furthermore, this study represents the first calculated coefficients of critical shear stress that correspond to numerical measurements of high vegetation. The implications of these data are crucial for improving stream restoration design and incorporating the use of remote sensing in assessing the impact of vegetation on stream bank strength. The increasing initiative for open-source data, and free access to cloud-based remote sensing and geospatial platforms such as Google Earth Engine®, dramatically increases user friendliness and allows similar studies to be readily conducted at low-cost by a wider range of users. Foremost, this approach saves users time that would otherwise be used to manually collect stream profiles, greatly enhancing the spatial coverage over-which these types of studies can be conducted.

REFERENCES

Abernethy B, Rutherfurd ID. 2001. The distribution and strength of riparian tree roots in relation to riverbank reinforcement.HydrologicalProcesses15: 63 – 79.

Andrews, E. D. (1983). Entrainment of gravel from naturally sorted riverbed material. *Geological Society of America Bulletin*, *94*, 1225-1231-undefined. http://pubs.geoscienceworld.org/gsa/gsabulletin/article-pdf/94/10/1225/3444767/i0016-7606-94-10-1225.pdf

ASCE Task Committee on Hydraulics, B. M. and M. of R. W. A. (1998). River Width Adjustment: Processes and Mechanisms by the ASCE Task Committee on Hydraulics, Bank Mechanics, and Modeling of River Width Adjustment. *Journal of Hydraulic Engineering*, *124*(9), 881–902. http://www.ascelibrary.org

Beeson, C. E., and P. F. Doyle. 1995. "Comparison of Bank Erosion at Vegetated and Non-vegetated Channel Bends." Journal of the American Water Resources Association 31, no. 6: 983-990. doi: 10.1111/j.1752-1688.1995.tb03414.x.

Childers, A., Brochure Committee, W., & Department of Natural Resources, M. (2010). *Resource Sheet 1: Streambank Erosion and Restoration*.

Coulston, J. W., G. G.Moisen, B. T.Wilson, M. V.Finco, W. B.Cohen, and C. K.Brewer . 2012. “Modeling Percent Tree Canopy Cover: A Pilot Study.” *Photogrammetric Engineering & Remote Sensing* 78 (7): 715–727. doi:10.14358/PERS.78.7.715

Doll, B. A., Grabow, G. L., Hall, K. R., Halley, J., Harman, W. A., Jennings, G. D., & Wise, D. E. (n.d.). *Stream Restoration: A Natural Channel Design Handbook*. Retrieved October 16, 2020, from https://semspub.epa.gov/work/01/554360.pdf

Fripp, J., Copeland, R., & Jonas, M. (2001). AN OVERVIEW OF THE USACE STREAM RESTORATION GUIDELINES. *Proceedings of the Seventh Federal Interagency Sedimentation Conference*, 1–8.

Gregory, K.J., and A.M. Gurnell, 1988. Vegetation and River Channel Form and Process. In: Biogeomorphology, H. Viles (Editor).Basil Blackwell, Oxford, pp. 11-42.

Griffin, A. M., Morgan, C. L. S., Nelson, R. F., & Tjoelker, M. (2006). *Using Lidar and Normalized Difference Vegetation Index to Remotely Determine LAI and Percent Canopy Cover at Varying Scales.*

Gubernick, R. A., Cenderelli, D. A., Bates, K. K., Johansen, D. K., & Jackson, S. D. (2008). *Stream Simulation: An Ecological Approach to Providing Passage for Aquatic Organisms at Road-Stream Crossings*.

Hey, R. D., & Thorne, C. R. (1986). Stable Channels with Mobile Gravel Beds. *Journal of Hydraulic Engineering*, *112*(8), 671–689.

Hopkinson, L., & Wynn, T. (2009). Vegetation impacts on near bank flow. *Ecohydrology*, *2*(4), 404–418. https://doi.org/10.1002/eco.87

Huang, H. Q., & Nanson, G. C. (1998). *The Influence of Bank Strength on Channel Geometry: an Integrated Analysis of some Observations* (Vol. 23).

Huang, H. Q., & Warner, R. F. (1995). The Multivariate Controls of Hydraulic Geometry: A Causal Investigation in terms of Boundary Shear Distribution. *Earth Surface Processes and Landforms* (Vol. 20).

Jang, C. L., & Shimizu, Y. (2007). Vegetation effects on the morphological behavior of alluvial channels. *Journal of Hydraulic Research*, *45*(6), 763–772. https://doi.org/10.1080/00221686.2007.9521814

Julian, J. P., & Torres, R. (2006). Hydraulic erosion of cohesive riverbanks. *Geomorphology*, *76*(1–2), 193–206. https://doi.org/10.1016/j.geomorph.2005.11.003

Julian, J. P. (2004). *Fluvial Erosion of Cohesive Riverbanks Sand River, SC*. University of South Carolina.

Klausmeyer, K. J. (2020). *United States Department of Agriculture Streambank Erosion Streambank Erosion*. https://www.nrcs.usda.gov/wps/portal/nrcs/detail/ks/newsroom/features/?cid=nrcs142p2_033508

Knighton, D. (1998). *Fluvial Forms and Processes: A New Perspective*.

Krzeminska, D., Kerkhof, T., Skaalsveen, K., & Stolte, J. (2019). Effect of riparian vegetation on stream bank stability in small agricultural catchments. *Catena*, *172*, 87–96. https://doi.org/10.1016/j.catena.2018.08.014

Lawler, D. M. (1995). *Effects of Scale on Interpretation and Management of Sediment and Water Quality* (Issue 226). IAHS Publ.

McCandless, T. L., & Everett, R. A. (2002). *Maryland Stream Survey: Bankfull Discharge and Channel Characteristics of Streams in the Piedmont Hydrologic Region Bankfull Discharge and Channel Characteristics of Streams in the Piedmont Hydrologic Region*. www.fws.gov/r5cbfo

Mccandless, T. L. (2003). Maryland Stream Survey: *Bankfull Discharge and Channel Characteristics of Streams in the Allegheny Plateau and the Valley and Ridge Hydrologic Regions.* www.fws.gov/r5cbfo

Pollen-Bankhead, N., & Simon, A. (2010). Hydrologic and hydraulic effects of riparian root networks on streambank stability: Is mechanical root-reinforcement the whole story? *Geomorphology*, *116*(3–4), 353–362. https://doi.org/10.1016/j.geomorph.2009.11.013

Rosgen, D. L. (1994). CATENA A classification of natural rivers. In *Catena* (Vol. 22).

Rosgen, D. (2011). *Natural Channel Design (NCD): Fundamental Concepts, Assumptions & Methods*.

Simon, A., & Collison, A. J. C. (2002). Quantifying the mechanical and hydrologic effects of riparian vegetation on streambank stability. *Earth Surface Processes and Landforms*, *27*(5), 527–546. https://doi.org/10.1002/esp.325

VanDersal, W. R. 1938. Native Woody Plants of the United States: Their Erosion-Control and Wildlife Values. Misc. publication No. 303. United States Department of Agriculture. Government Printing Office, Washington, D. C.

Yu, G. A., Li, Z., Yang, H., Lu, J., Huang, H. Q., & Yi, Y. (2020). Effects of riparian plant roots on the unconsolidated bank stability of meandering channels in the Tarim River, China. *Geomorphology*, *351*. https://doi.org/10.1016/j.geomorph.2019.10

APPENDIX A

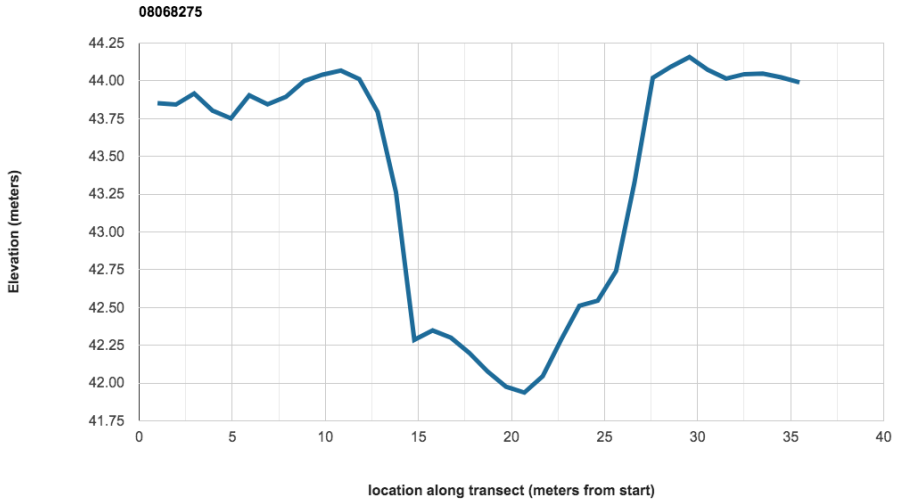

Figure 18. Stream profile collected using a DEM at USGS station 0806275. From this profile, width, depth, cross-sectional area, and wetted perimeter were calculated.

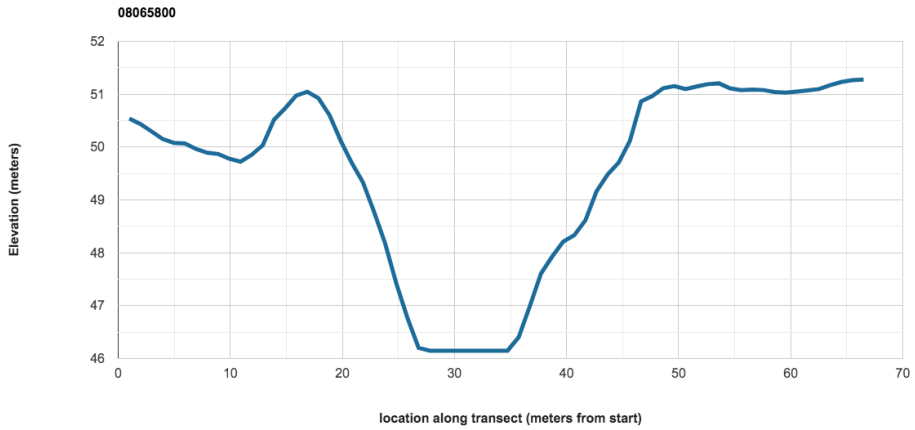

Figure 19. Stream profile collected using a DEM at USGS station 08065800. From this profile, width, depth, cross-sectional area, and wetted perimeter were calculated.

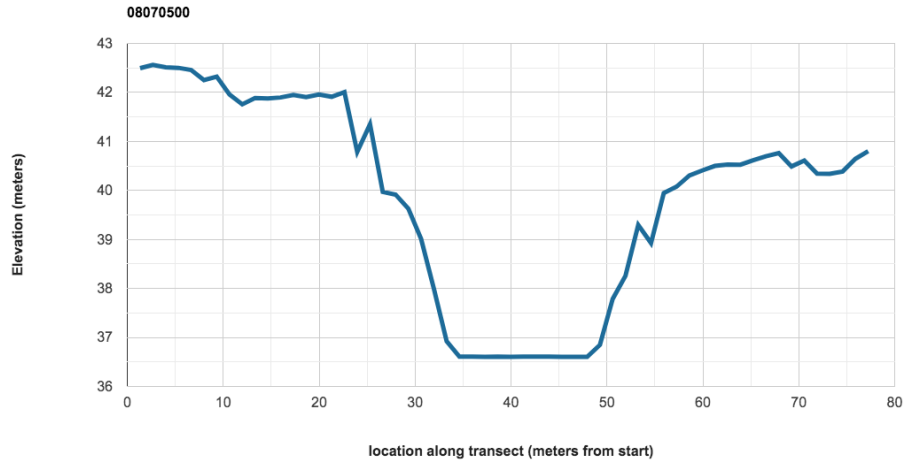

Figure 20. Stream profile collected using a DEM at USGS station 08070500. From this profile, width, depth, cross-sectional area, and wetted perimeter were calculated.

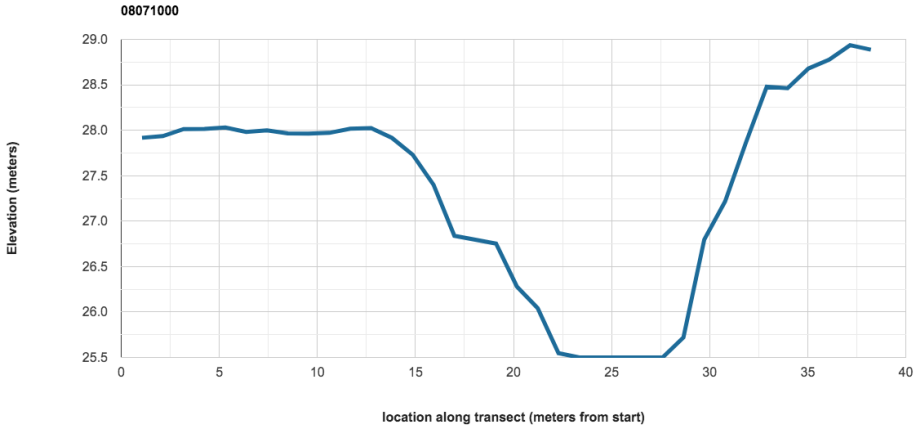

Figure 21. Stream profile collected using a DEM at USGS station 08071000. From this profile, width, depth, cross-sectional area, and wetted perimeter were calculated.

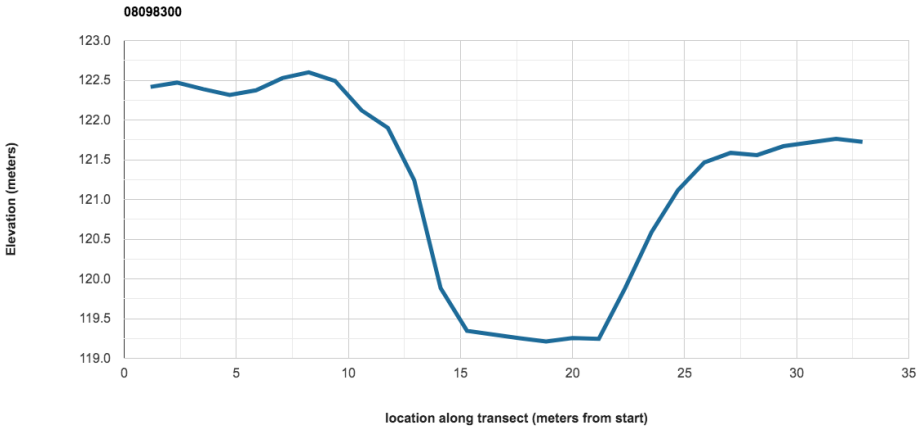

Figure 22. Stream profile collected using a DEM at USGS station 08098300. From this profile, width, depth, cross-sectional area, and wetted perimeter were calculated.

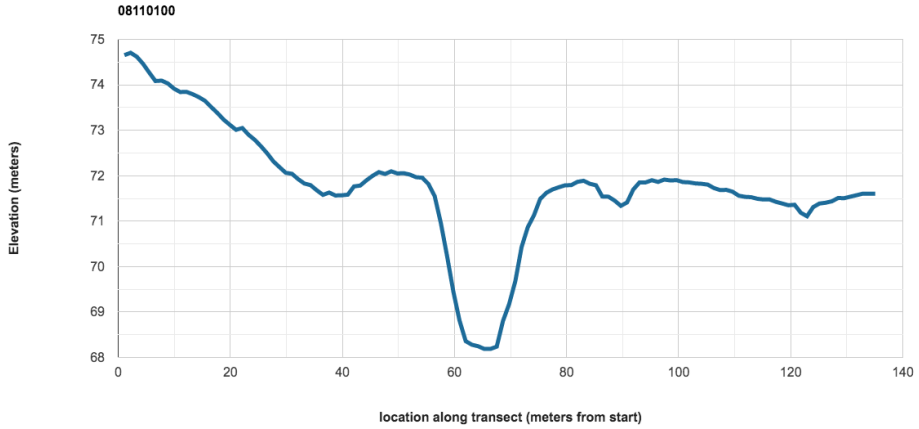

Figure 23. Stream profile collected using a DEM at USGS station 08110100. From this profile, width, depth, cross-sectional area, and wetted perimeter were calculated.

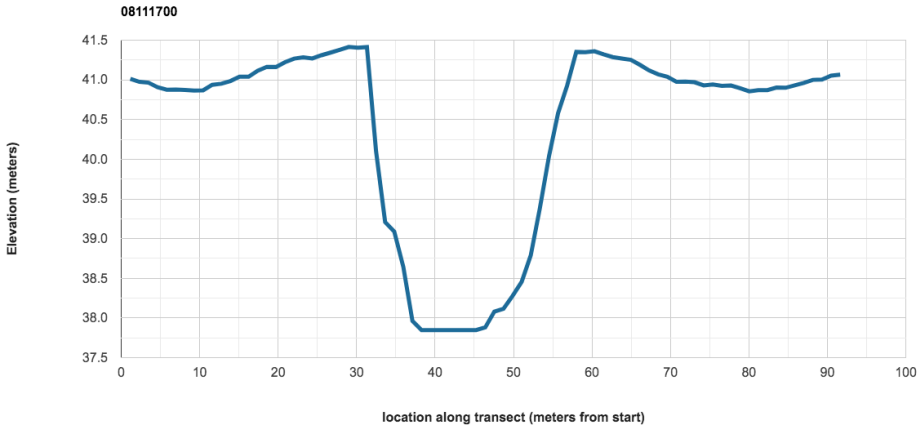

Figure 24. Stream profile collected using a DEM at USGS station 08111700. From this profile, width, depth, cross-sectional area, and wetted perimeter were calculated.

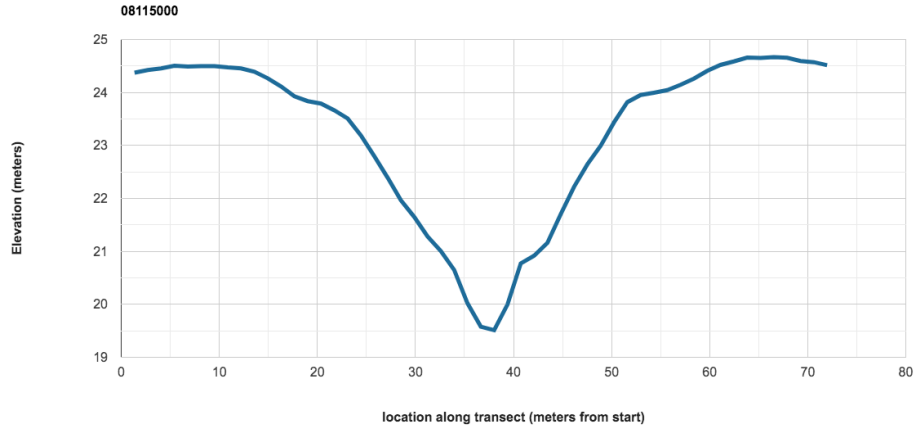

Figure 25. Stream profile collected using a DEM at USGS station 08115000. From this profile, width, depth, cross-sectional area, and wetted perimeter were calculated.

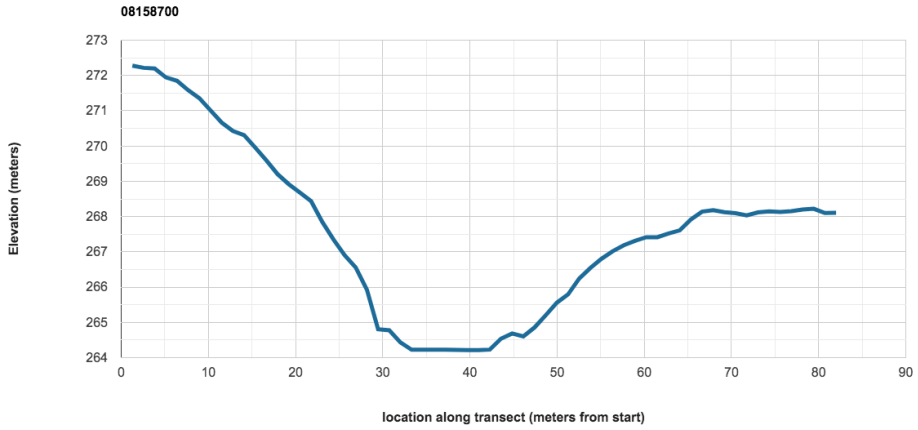

Figure 26. Stream profile collected using a DEM at USGS station 08158700. From this profile, width, depth, cross-sectional area, and wetted perimeter were calculated.

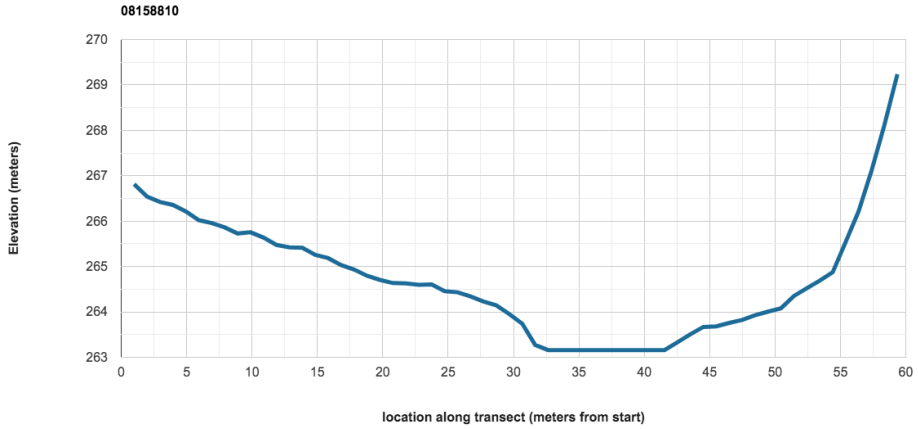

Figure 27. Stream profile collected using a DEM at USGS station 08158810. From this profile, width, depth, cross-sectional area, and wetted perimeter were calculated.

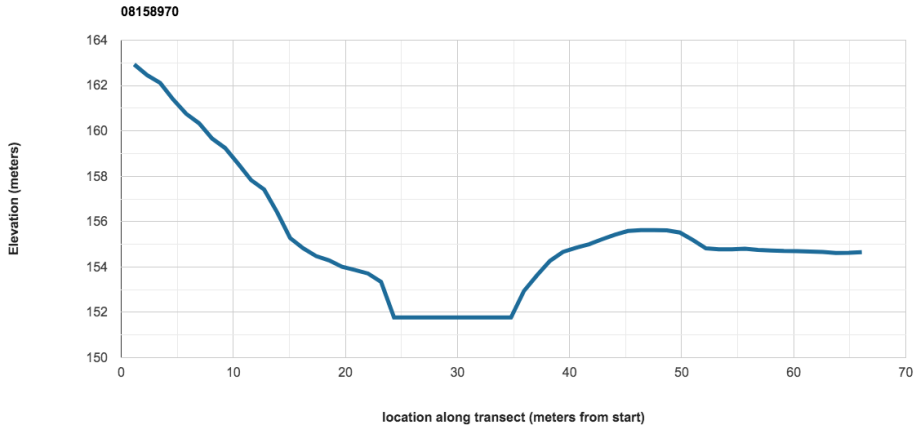

Figure 28. Stream profile collected using a DEM at USGS station 08158970. From this profile, width, depth, cross-sectional area, and wetted perimeter were calculated.

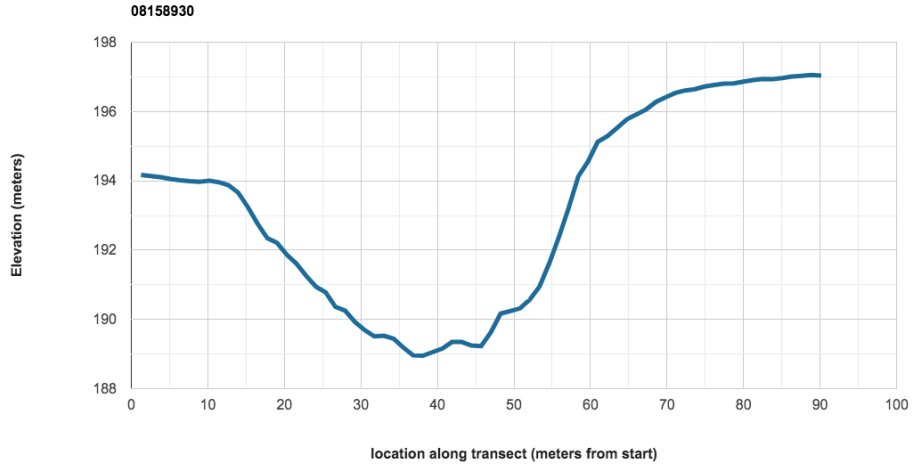

Figure 29. Stream profile collected using a DEM at USGS station 08158930. From this profile, width, depth, cross-sectional area, and wetted perimeter were calculated.

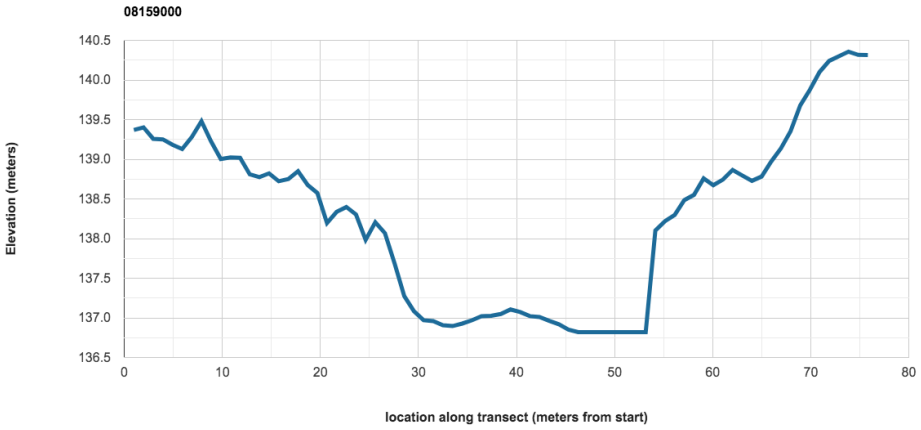

Figure 30. Stream profile collected using a DEM at USGS station 08159000. From this profile, width, depth, cross-sectional area, and wetted perimeter were calculated.

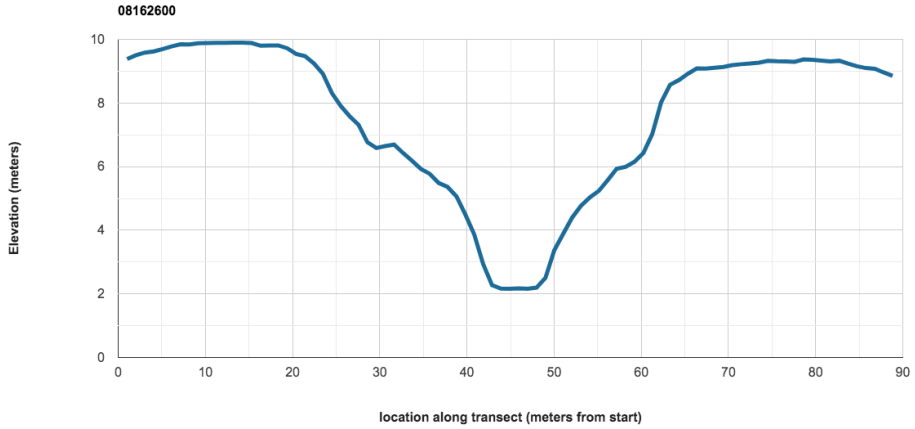

Figure 31. Stream profile collected using a DEM at USGS station 08162600. From this profile, width, depth, cross-sectional area, and wetted perimeter were calculated.

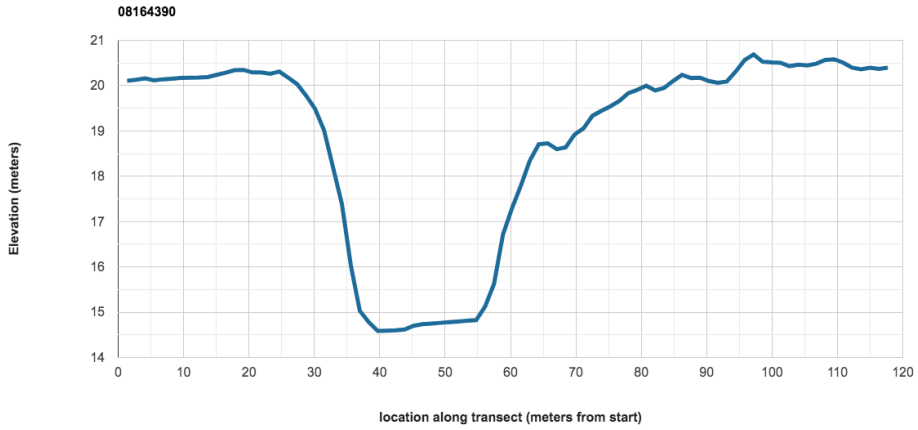

Figure 32. Stream profile collected using a DEM at USGS station 08164390. From this profile, width, depth, cross-sectional area, and wetted perimeter were calculated.

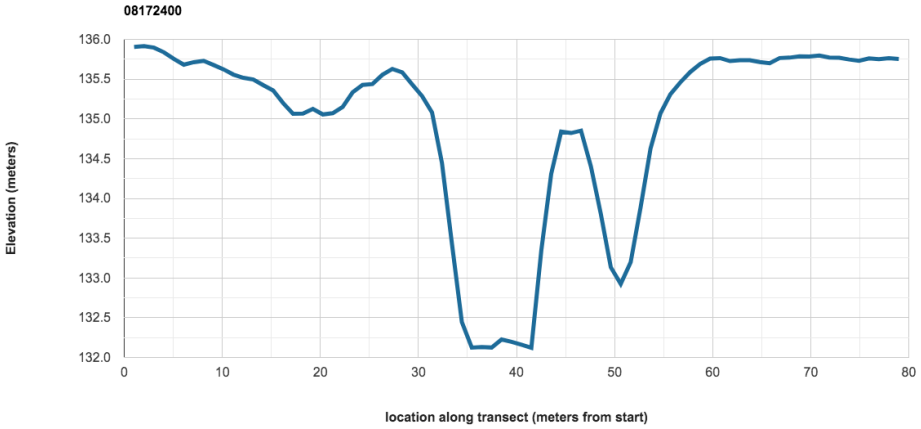

Figure 33. Stream profile collected using a DEM at USGS station 08172400. From this profile, width, depth, cross-sectional area, and wetted perimeter were calculated.

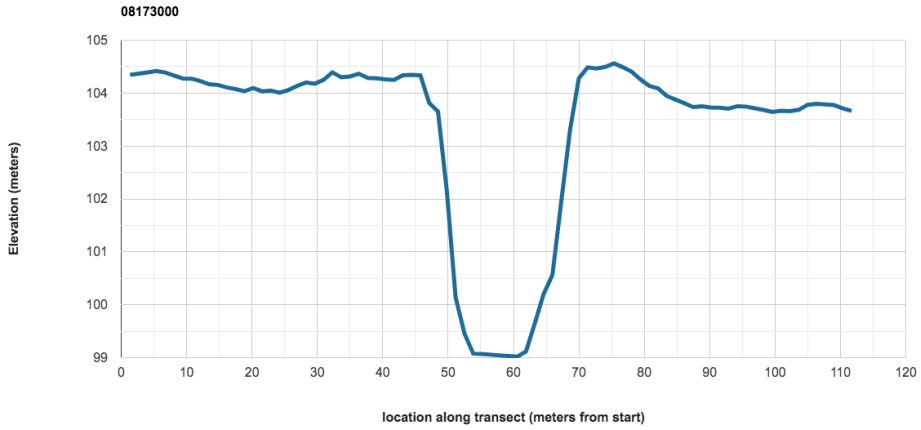

Figure 34. Stream profile collected using a DEM at USGS station 08173000. From this profile, width, depth, cross-sectional area, and wetted perimeter were calculated.

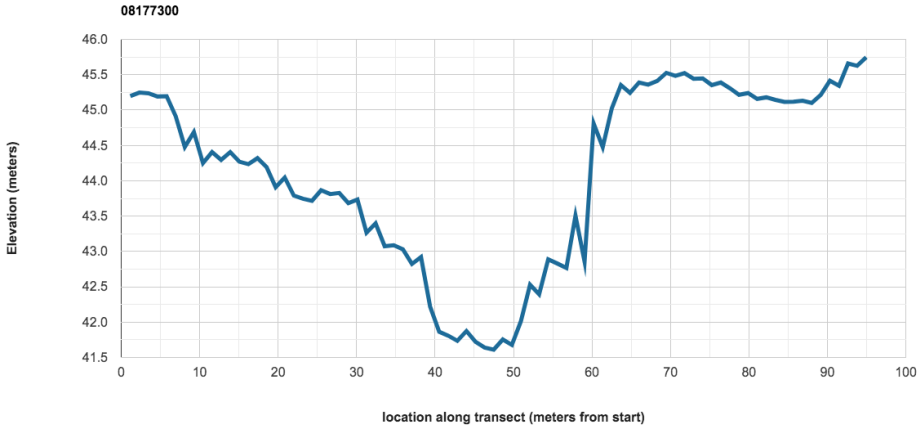

Figure 35. Stream profile collected using a DEM at USGS station 08177300. From this profile, width, depth, cross-sectional area, and wetted perimeter were calculated.

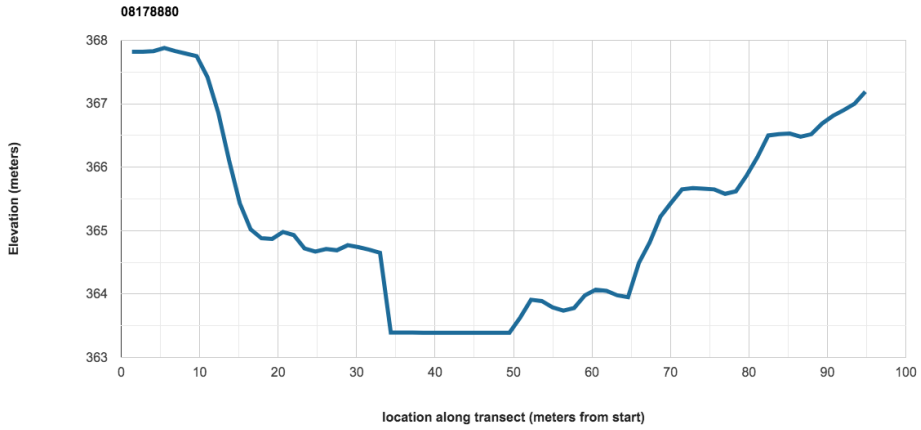

Figure 36. Stream profile collected using a DEM at USGS station 08178880. From this profile, width, depth, cross-sectional area, and wetted perimeter were calculated.

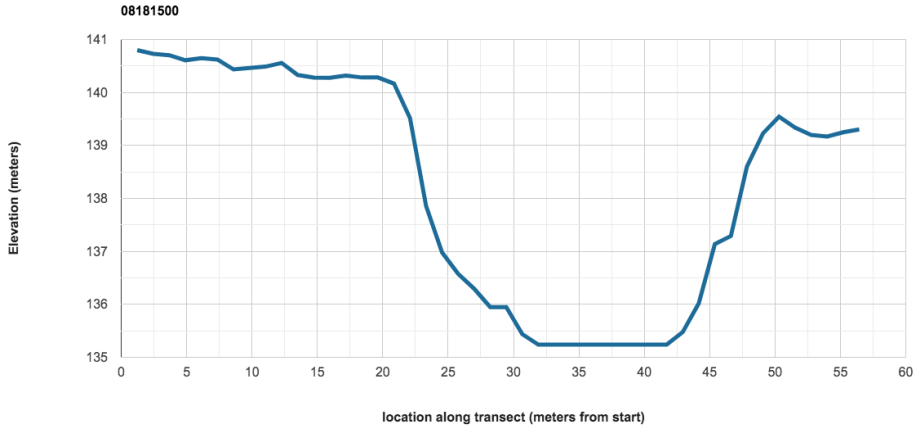

Figure 37. Stream profile collected using a DEM at USGS station 08181500. From this profile, width, depth, cross-sectional area, and wetted perimeter were calculated.

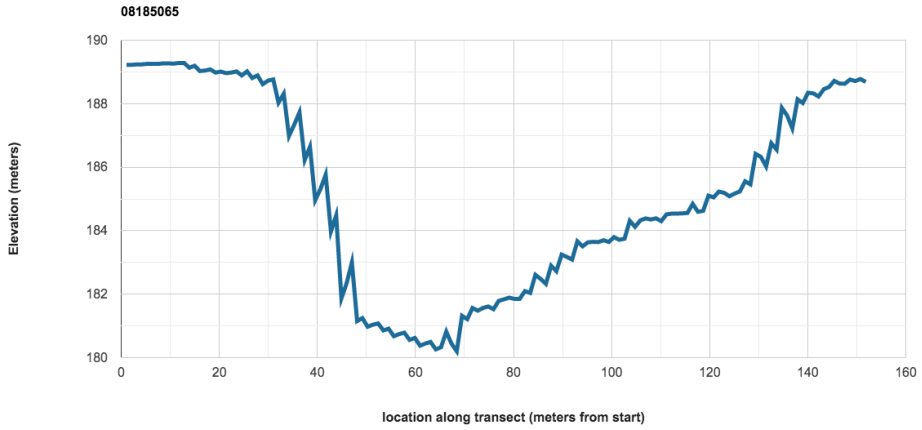

Figure 38. Stream profile collected using a DEM at USGS station 08185065. From this profile, width, depth, cross-sectional area, and wetted perimeter were calculated.

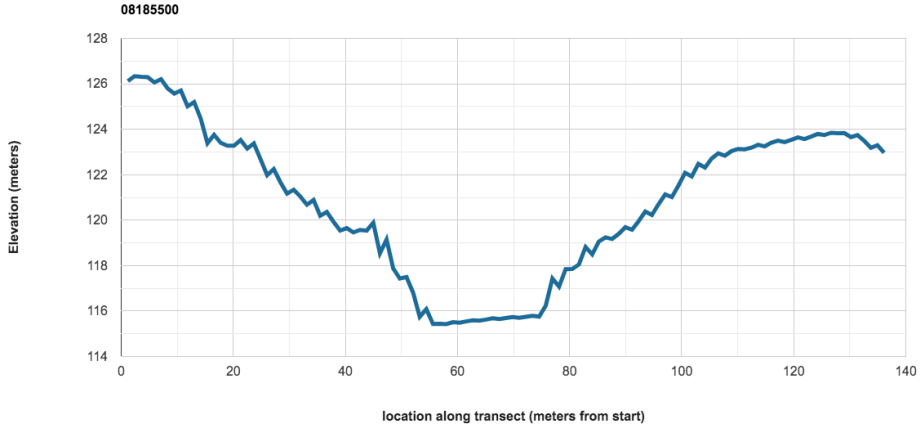

Figure 39. Stream profile collected using a DEM at USGS station 08185500. From this profile, width, depth, cross-sectional area, and wetted perimeter were calculated.

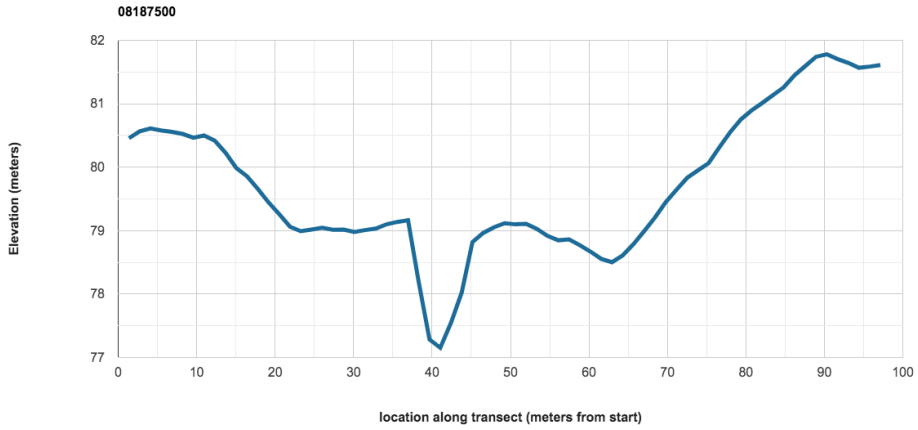

Figure 40. Stream profile collected using a DEM at USGS station 08187500. From this profile, width, depth, cross-sectional area, and wetted perimeter were calculated.

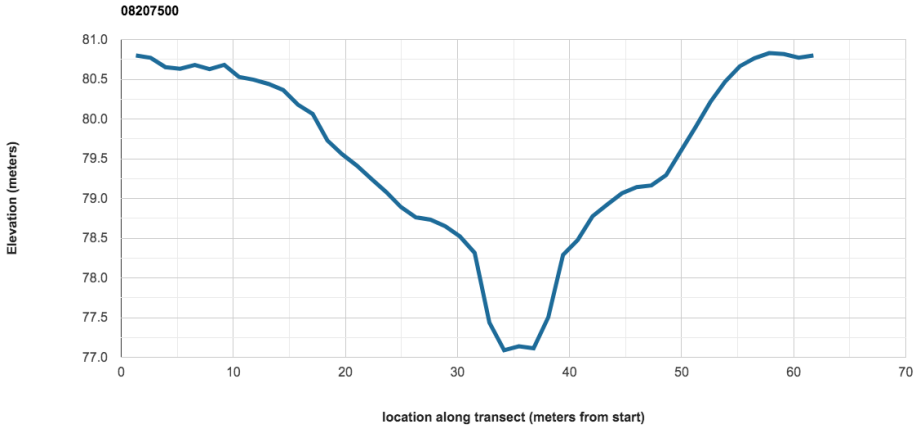

Figure 41. Stream profile collected using a DEM at USGS station 08207500. From this profile, width, depth, cross-sectional area, and wetted perimeter were calculated.

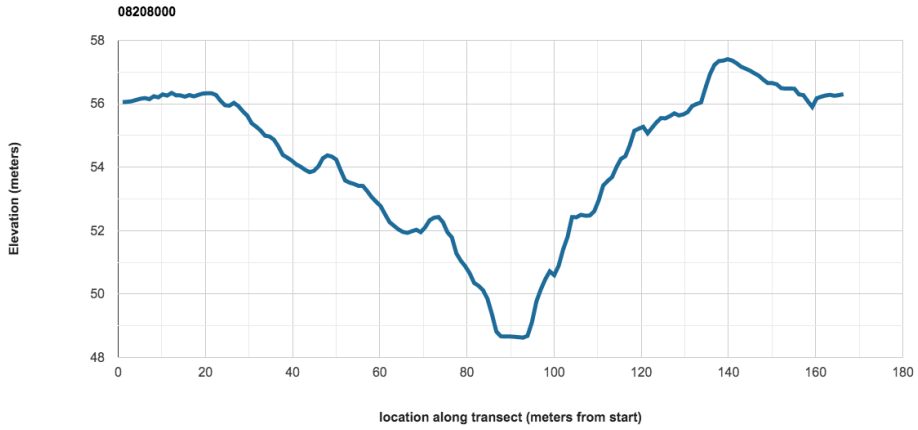

Figure 42. Stream profile collected using a DEM at USGS station 08202000. From this profile, width, depth, cross-sectional area, and wetted perimeter were calculated.

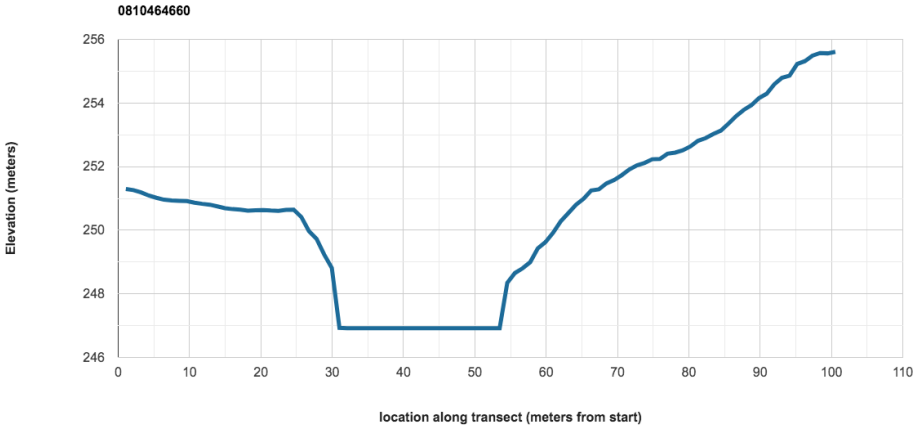

Figure 43. Stream profile collected using a DEM at USGS station 0810464660. From this profile, width, depth, cross-sectional area, and wetted perimeter were calculated.

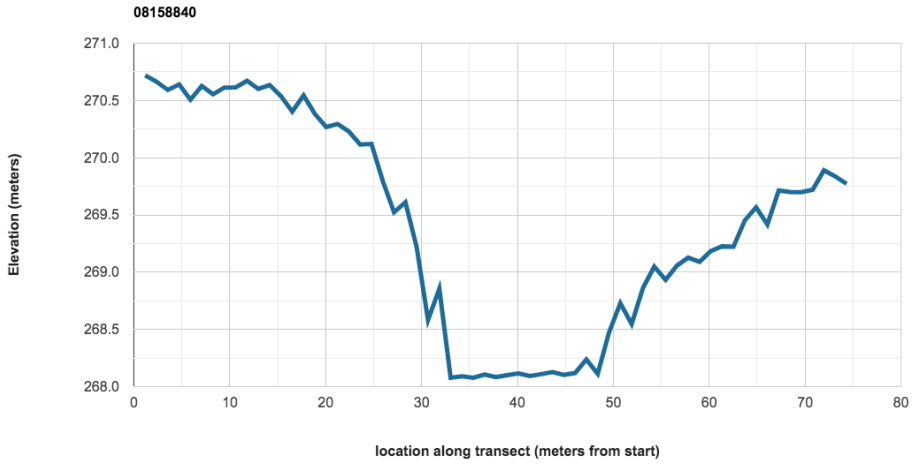

Figure 44. Stream profile collected using a DEM at USGS station 08158840. From this profile, width, depth, cross-sectional area, and wetted perimeter were calculated.

Table 5. Chart summarizing all the dominant soil type, lithology, river basin, and county for all stations used in this study.

Station	Hydrol-ogic Soil Group	Soil Description	County	Basin	Lithology
08065800	C/D	clay loam	madison	Trinity	Sand
08070500	A	fine sandy loam	montgomery	San Jacinto	Sand
08098300	D	clay	milam	Brazos	Clay or Mud
0810464660	B	silty clay loam	williamson	Brazos	Terrace
08110100	D	clay	burleson	Brazos	Sand
08111700	D	clay	Austin	Brazos	Sand
08115000	D	clay	fort bend	Brazos	Clay or Mud
08158700	B	silty clay loam	hays	Colorado	Limestone
08158810	B	silty clay	hays	Colorado	Limestone
08158860	A	stratified very gravelly coarse sand to very gravelly sand	travis	Colorado	Sand
08158970	B	silty clay loam	travis	Colorado	Clay or Mud
08159000	A	stratified very gravelly coarse sand to very gravelly sand	travis	Colorado	Clay or Mud
08164390	C	clay, sandy clay loam	jackson	Lavaca	Sand
08172400	D	clay	Caldwell	Guadalupe	Sand
08173000	D	clay	caldwell	Guadalupe	Sand
08177300	A	sand, fine sand	goliad	Guadalupe	Clay or Mud
08178880	A	gravelly sandy loam	bandera	San Antonio	Limestone
08181500	B	clay loam	bexar	San Antonio	Terrace
08185065	D	clay	bexar	San Antonio	Terrace
08185500	A	fine sandy loam	wilson	San Antonio	Terrace
08187500	D	clay	karnes	San Antonio	Sand
08189300	A	fine sandy loam	bee	San Antonio-Nueces	Terrace
08207500	A	loamy fine sand	atascosa	Nueces	Sand
08208000	D	clay	live oak	Nueces	Sand
08210400	A	fine sandy loam	live oak	Nueces	Clay or Mud

Table 6. Chart summarizing the bankfull discharge and bankfull depth collected for each USGS station. The percent difference in depth corresponds to the difference between the modeled bankfull depth and the most accurate depth that could be extracted from the generated stream profile

Station	Bankfull Discharge (cms)	Bankfull Depth (m)	Bankfull Width	τ_{cbk}
08158930	17.01	1.8788	29.2	0.000460
08070500	33.7	4.07	20.3	0.002822
08065800	79.6	5.31	62.2	0.000220
08068275	45.9	3.73	24.4	0.002475
08098300	31.1	3.66	58.7	0.001052
0810464660	19.7	1.81	47.4	0.000031
08110100	25.9	3.91	41.4	0.005411
08115000	47.0	5.64	28.2	0.001038
08158700	49.8	2.06	66.4	0.000133
08158810	2.6	1.10	20.2	0.000036
08158840	2.3	1.44	25.1	0.000068
08158860	5.5	0.87	26.3	0.000003
08158930	17.0	1.88	29.2	0.000459
08158970	17.5	2.54	39.1	0.000038
08159000	41.6	2.68	41.0	0.001211
08162600	69.7	6.34	36.4	0.000070
08164390	71.4	5.45	50.3	0.000726
08173000	64.6	5.58	46.6	0.000127
08177300	3.6	2.17	13.6	0.000402
08178880	5.1	1.49	19.2	0.028591
08181500	41.6	3.83	25.1	0.001747
08185065	2.5	3.28	25.8	0.011340
08185500	235.7	3.71	25.6	0.001136
08187500	13.2	3.81	74.3	0.000145
08189300	10.3	2.98	80.6	0.000038
08207500	6.6	3.64	54.6	0.000057
08208000	43.3	4.20	49.3	0.000408
08210400	0.3	1.98	34.4	0.000579

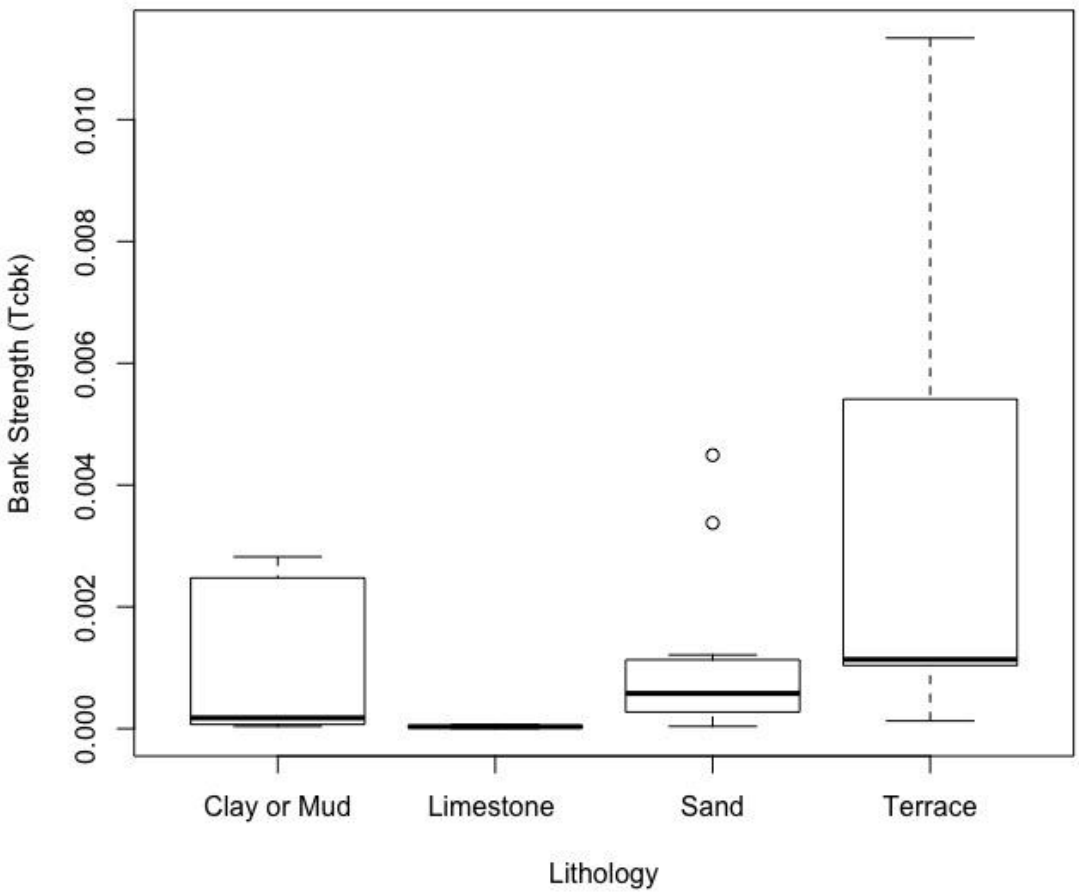

Figure 45. Box plot of bank strength calculations (τ_{cbk}) as separated by lithology. Two outliers (stations 08111700 and 08172400) were removed from the sand group.

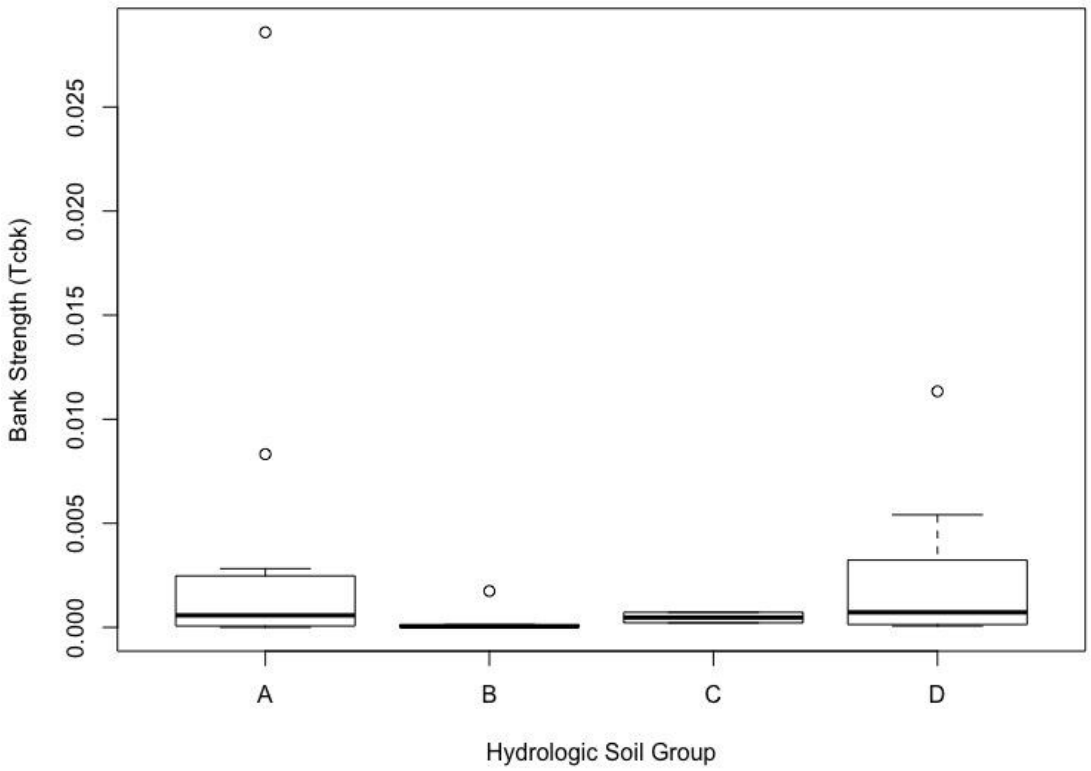

Figure 46. Distribution of bank strengths and the corresponding soil group found at each station location.

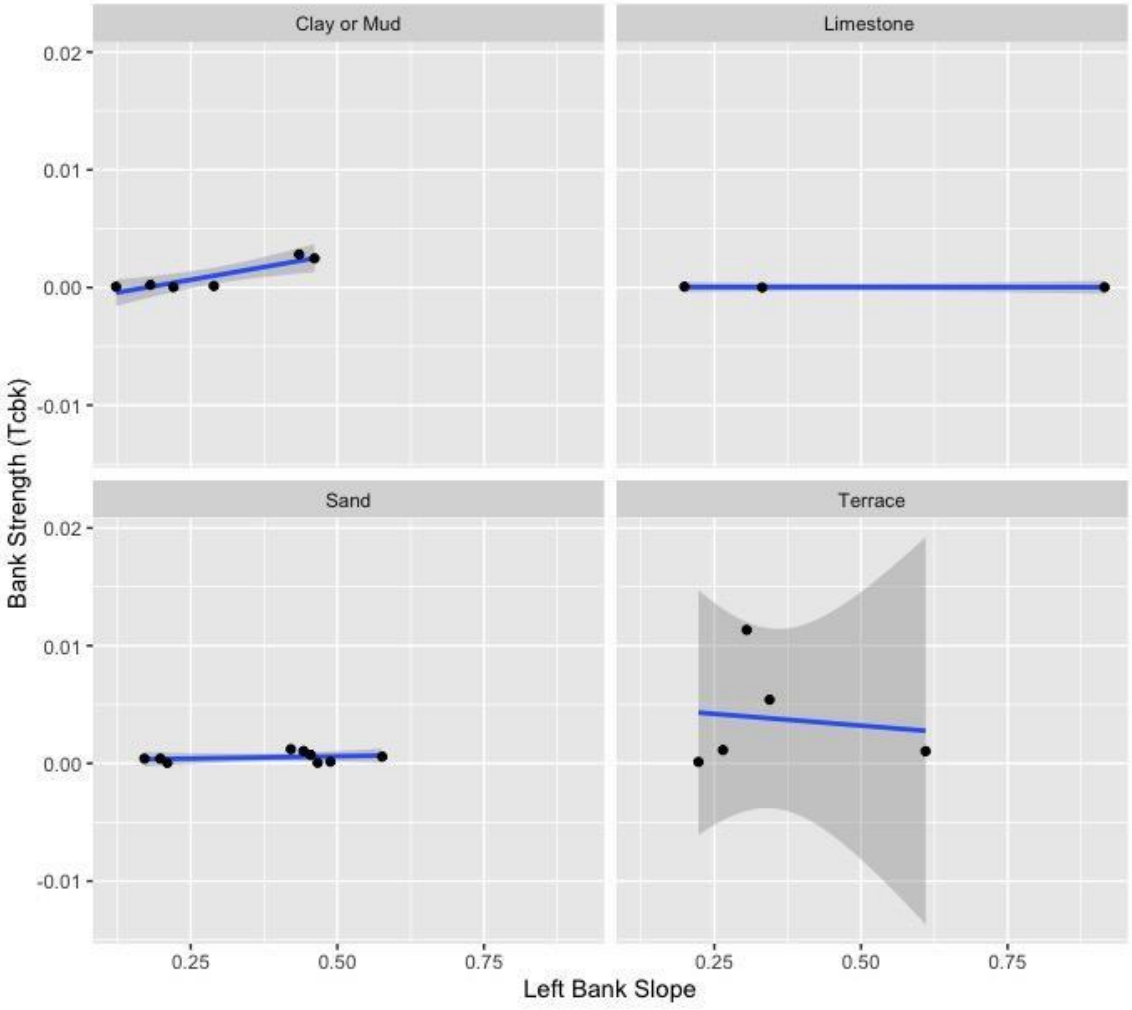

Figure 47. Plots of the left bank slopes along the stream bank profiles as they relate to the associated bank strength. Left bank slopes generally increase with increasing bank strength in clay streams. The relationship is less defined with sand streams. There is a loose negative relationship in terrace streams. Slopes in limestone streams have no noticeable effect on bank strength.

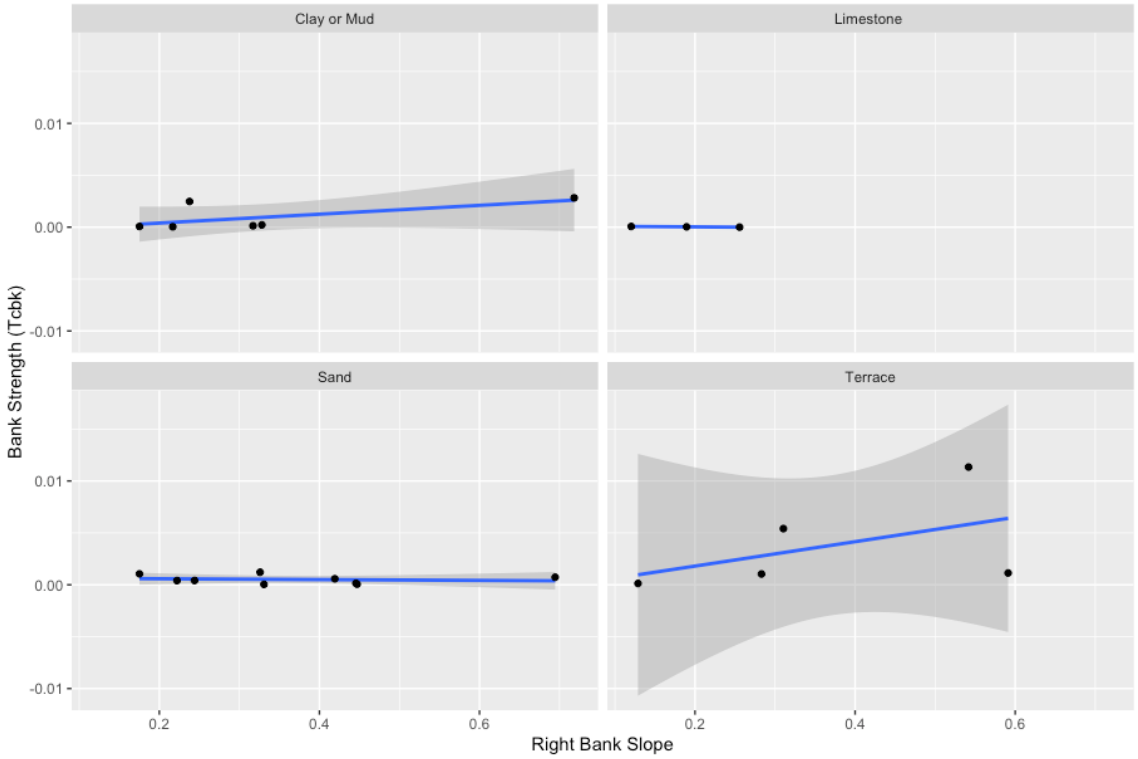

Figure 48. Plots of the right bank slopes along the stream bank profiles as they relate to the associated bank strength. Right bank slopes generally increase with increasing bank strength in clay streams. The relationship is loosely negative in sand streams. There is a loose positive relationship in terrace streams. Right bank slopes in limestone streams have no noticeable effect on the bank strength.

Table 7. Width and depth measurements of the Google Earth Engine ® generated stream profiles compared with field measurements at the same location.

Station	Width (m)	% difference in Width	Depth (m)	% difference in Depth
GEE 1	10.6	22.5%	1.47	2.57%
Field 1	8.22		1.43	
GEE 2	14.9	34.9%	2.41	3.81%
Field 2	9.75		2.32	
GEE 3	9.89	35.3%	0.901	12.2%
Field 3	6.48		1.01	

Table 8. Calculated coefficients for varying percent volume of vegetation for high vegetation.

lithology	bank vegetation	Tcbk	Tfactor	Toverall	Tc coeff
clay or mud	0%	0.000133	1	1	1
	20%	0.002475	18.592	18.592	14.6
	30%	0.000459	3.451	3.451	15.4
	40%	0.002822	21.194	21.194	20.0
sand	0%	0.000038	1	0.986	
	20%	0.000408	10.768	10.621	
	30%	0.001052	27.739	27.362	
	40%	0.000726	19.126	18.866	
		20%	**30%**	**40%**	**average**
		1.73	0.12	1.11	0.99

APPENDIX B

All the relevant code used to generate the stream profile can be found at:

https://code.earthengine.google.com/f3f29f01227af83f7c8d66a4f2895805

The code used to collect PVVs can be found at:

https://code.earthengine.google.com/9265798443ea28c99e79d13d5942e9ee